STRUCTURAL OPTIMIZATION FOR RELIABILITY USING NONLINEAR GOAL PROGRAMMING

IN-38

Final Report NASA Grant
NAG1 - 1837

By

Dr. Mohamed E. El-Sayed

Professor of Mechanical Engineering
Kettering University

May 30, 1999

This research was conducted at NASA Langley Research Center

ABSTRACT

This report details the development of a reliability based multi-objective design tool for solving structural optimization problems. Based on two different optimization techniques, namely sequential unconstrained minimization and nonlinear goal programming, the developed design method has the capability to take into account the effects of variability on the proposed design through a user specified reliability design criterion. In its sequential unconstrained minimization mode, the developed design tool uses a composite objective function, in conjunction with weight ordered design objectives, in order to take into account conflicting and multiple design criteria. Multiple design criteria of interest including structural weight, load induced stress and deflection, and mechanical reliability. The nonlinear goal programming mode, on the other hand, provides for a design method that eliminates the difficulty of having to define an objective function and constraints, while at the same time has the capability of handling rank ordered design objectives or goals.

For simulation purposes the design of a pressure vessel cover plate was undertaken as a test bed for the newly developed design tool. The formulation of this structural optimization problem into sequential unconstrained minimization and goal programming form is presented. The resulting optimization problem was solved using: (i) the linear extended interior penalty function method algorithm; and (ii) Powell's conjugate directions method. Both single and multi-objective numerical test cases are included demonstrating the design tool's capabilities as it applies to this design problem.

ACKNOWLEDGEMENT

The author acknowledges the support given to his graduate student Mr. Michael Edghill during his stay at NASA Langley research center. Sincere thanks to Dr. Jerrold Housner, Dr. Christopher Sandridge, Michael Riley, Danniella Muhiem, David Sleigh, and Crystal Carr for their help and support.

TABLE OF CONTENTS

LIST OF FIGURES

LIST OF TABLES AND PHOTOGRAPHS

LIST OF TABLES

LIST OF PHOTOGRAPHS

NOMENCLATURE

Symbol	Description	Units
A	Area	mm^2
D	Inside diameter	mm
d	Inside diameter of shell	in.
E	Modulus of elasticity, Efficiency	GPa
e	Natural base	
e_i	ith residual	
h	Thickness	mm
I	Integral	
P	Internal design pressure	psi
P_{max}	Maximum internal pressure	MPa
R	Observed reliability	
R_o	Target reliability	
S	Maximum allowable stress, Strength	psi MPa
S_{ut}	Ultimate tensile strength	MPa
S_y	Yield strength	MPa
t	Minimum required thickness	in.
W	Structural weight	kg
W_o	Target structural weight	kg
x_i	ith predictor	
y_i	ith response	
z	Load induced deflection	mm
z_{max}	Maximum allowable deflection, Maximum observed deflection	mm mm

z	Standard normal variate	
β_o	Regression parameter	
β_1	Regression parameter	
$\mu_{Y\|x}$	Mean value of Y at x	
μ_s	Mean strength	MPa
μ_σ	Mean stress	MPa
ν	Poisson's ratio	
ρ	Density	kg/mm^3
σ	Maximum principal stress, Load induced stress	MPa MPa
σ_{max}	Maximum allowable stress, Maximum observed stress	MPa MPa
$\hat{\sigma}_s$	Strength standard deviation	MPa
$\hat{\sigma}_\sigma$	Stress standard deviation	MPa

CHAPTER I. INTRODUCTION

The concept of optimization is intrinsically tied to the engineering design process. The desire to develop and manufacture a product that is of superior performance and reliability than its predecessor is a major driving force in engineering design. As a result, design tools that allow the attainment of these goals in a timely and economical fashion have become essential in the design process. Over the past forty years the development of numerical optimization techniques has been instrumental in this context.

Since the pioneering work by Schmit in 1960, the use of numerical optimization techniques in engineering design has gained widespread acceptance and popularity [1]. In the spirit of this work and that which has followed since [2] lies the motivation for the work in this paper. In particular, this thesis was conceived having as its primary objective to develop a reliability based multi-objective design tool. A tool that should have the capability to take into account the effects of variability on the proposed design, while at the same time provides a realistic design model that takes into account conflicting and multiple objectives. Multiple objectives of interest that include structural weight, load induced stress and deflection, and mechanical reliability.

As a testbed for this newly developed design tool, the design of a pressure vessel cover plate was selected. In the proceeding sections, a brief insight into the design of pressure vessels, namely categories, code of standards, and welding method(s) is presented for reference. A brief review of previous work in structural optimization follows. This chapter concludes with an outline of the work in this thesis.

1.1 Pressure Vessel Design

Categories

The design of a pressure vessel, and as a consequence its components (e.g. cover plates, nozzles, etc.), is inevitably determined by its intended use. In essence, function ultimately dictates the appropriate design. In the case of industrial applications (i.e. hydrocarbon processing), pressure

vessels fall into three broad categories, namely drums, towers, and reactors [3]. Each category is associated with a specific application. For instance, drums are primarily used for separating or mixing fluids and in general are thin-wall vessels made of carbon steel [3]. If service conditions warrant it, drums may be thick-walled vessels and a low alloy steel may be employed given its corrosion resistance [3].

Towers, on the other hand, are used for distillation, absorption or stripping and are routinely operated at modest temperature and pressures [3]. Given their harsh operating environment, towers are commonly clad (coated) with ferritic or austenitic stainless steel for added corrosion protection [3]. However, for extremely corrosive environments alloys such as molybdenum and chromium are generally required, and vessels made of special anti-corrosion materials such as titanium or zirconium are not uncommon [4]. In Photo 1, a pair of titanium pressure vessels are shown ready for final shipment and a lifetime of corrosive duty.

Photo 1. Titanium Grade 2 Pressure Vessels 84" OD [5]

Finally, this brief insight into industrial type pressure vessels concludes with the work-horses of industry, namely reactors. Not surprisingly, these vessels form the backbone of all industrial processes for in them the essential chemical reactions necessary for a wide range of applications take place [3]. In particular, in the oil and farming industries typical applications include[4]:

- For Oil Refineries
  - heavy oil, light oil desulphurization reactors
  - heavy oil hydrocracking reactors
- For Fertilizer Plants
  - urea reactors
  - ammonia converters

The elevated temperature and pressure at which reactors operate at commonly warrant the use of a thick-walled design. As a consequence, reactors may be solid wall or multi-layered [3]. Inherently, the multilayer design has various advantages over the solid wall design. Most notably is the fact that a multilayer design, as characterized by a thin laminate of thin plates, has better notch-ductility and by nature is less prone to brittle failure [3]. Nonetheless, most reactors continue to this day to be of a solid wall construction [3]. In Photo 2, a multilayer pressure vessel is shown during final inspection.

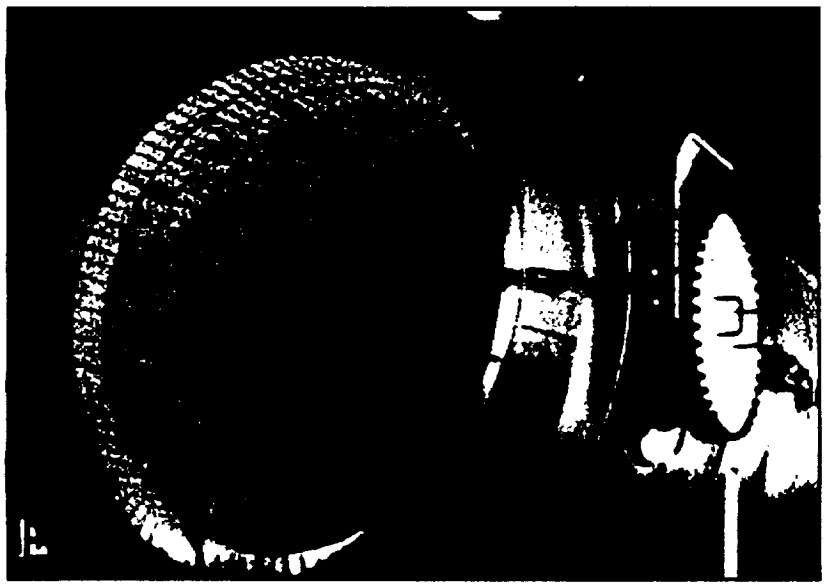

Photo 2. Pressure Vessel: Multilayer [6]

Lastly, it should be noted that with few exceptions the heads or cover plates of all industrial type pressure vessels are of a solid wall construction [3]. For high pressures the head is generally of a hemispherical design, however, configurations with flat, elliptical or torispherical heads are not uncommon [7].

ASME Boiler and Pressure Vessel Code

Enacted in 1914 after a disastrous boiler explosion in a shoe factory in Massachusetts, the ASME Boiler and Pressure Vessel Code has evolved over the years into a set of standards governing the design and construction of all pressure vessels in the United States [8]. Vessels designed, fabricated, and inspected under its provisions are ensured to meet/comply with the highest standards of safety in industry worldwide [3].

Of course, since 1914 the code has routinely been updated and new provisions added as advancements in materials, construction, methods of fabrication, and inspection were developed. Today, the ASME Code is composed of eleven sections and is listed here for reference.

ASME Boiler and Pressure Vessel Code [8]

- Section I. Power Boilers
- Section II. Material Specifications
    - Ferrous Materials, Part A
    - Nonferrous Materials, Part B
    - Welding Rods, Electrodes, and Filler Metals, Part C
    - Properties, Part D
- Section III, Division 1. Nuclear Power Plant Components
  Subsection NCA: General Requirements
  Subsection NB: Class 1 Components
  Subsection NC: Class 2 Components
  Subsection ND: Class 3 Components
  Subsection NE: Class MC Components
  Subsection NF: Component Supports
  Subsection NG: Core Support Structures
- Section III, Division 2. Concrete Reactor Vessel Containments
- Section IV. Heating Boilers
- Section V. Nondestructive Examinations

- Section VI. Recommended Rules for Care and Operation of Heating Boilers
- Section VII. Recommended Rules for Care of Power Boilers
- Section VIII, Division 1. Pressure Vessels
- Section VIII, Division 2. Pressure Vessels - Alternative Rules
- Section IX. Welding and Brazing Qualifications
- Section X. Fiberglass-Reinforced Plastic Pressure Vessels
- Section XI. Rules for Inservice Inspection of Nuclear Power Plant Components

Pertinent to pressure vessel design, the ASME Code provides a set of standard formulas used to compute the minimum required wall thickness. Formulas are also provided for vessel components such as cover plates (heads) and nozzles. Of interest in this regard is the minimum required thickness of a circular flat head given its importance, as will be seen later, in addressing the main objectives of this thesis. As defined per ASME Code UG-34 [9], the appropriate formula for a circular flat head is given by

$$t = d\sqrt{0.13\,P/SE} \qquad (1\text{-}1)$$

where:

t = minimum required thickness, exclusive of corrosion allowance, in.
d = inside diameter of shell, in.
P = internal design pressure, psi
S = maximum allowable stress value of material, psi
E = joint efficiency

In closing, it should be noted that the joint efficiency is a correction factor intended to take into account the quality of the weld between the shell (body) and cover plate (head) of the pressure vessel. In particular, the joint efficiency is a function of three factors, namely the type and design of the welded joint and the degree of examination [9]. In this context, type refers to whether a single or double butt or fillet weld will be employed. Provisions for the use of a backing strip are also addressed and ASME Code UW-12 [9] is listed here for reference.

The design of the welded joint, on the other hand, refers to whether, for example, a longitudinal or circumferential weld is required. In Figure 1, a schematic of a pressure vessel is shown illustrating the location and design of welded joints consistent with the provisions provided for in the ASME Code.

Lastly, the joint efficiency is also a function of the degree of examination the welded joint is subject to. As defined per the ASME Code, radiography and/or ultrasonic testing may be required for the examination of main seams [3]. Depending on the degree of examination, ranging from 100% radiography and ultrasonic testing to spot or even no examination, the Code provides a complete listing of the maximum allowable joint efficiencies to be used. The interested reader is referred to ASME Code Section UW-12 [9] for further details on this subject.

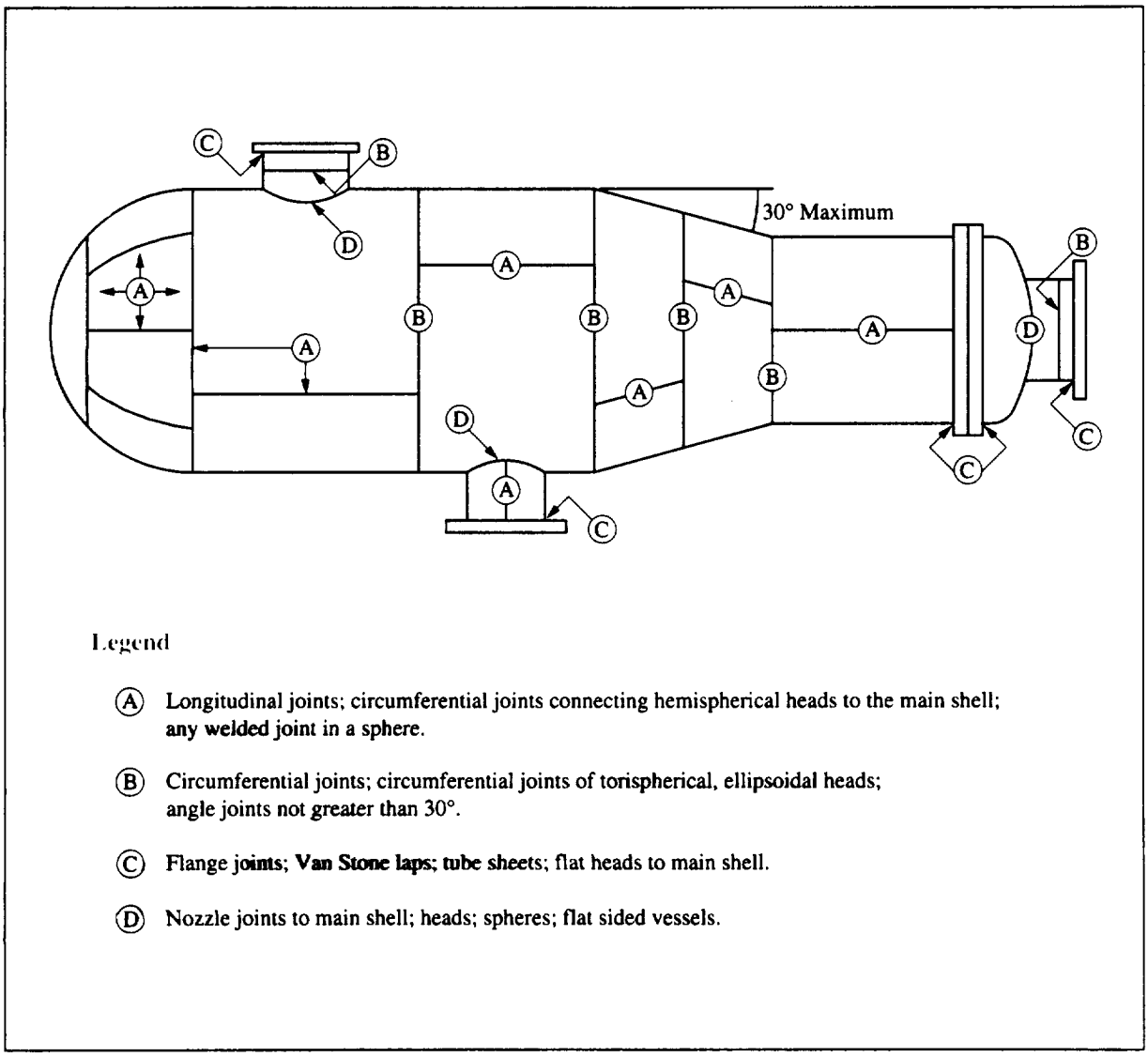

Legend

(A) Longitudinal joints; circumferential joints connecting hemispherical heads to the main shell; any welded joint in a sphere.

(B) Circumferential joints; circumferential joints of torispherical, ellipsoidal heads; angle joints not greater than 30°.

(C) Flange joints; Van Stone laps; tube sheets; flat heads to main shell.

(D) Nozzle joints to main shell; heads; spheres; flat sided vessels.

Figure 1. Welded Joint Categories and Locations [8]

Welding

The fusion welding processes most appropriate to pressure vessel manufacture are shielded metal arc welding and submerged arc welding [3]. For brevity and given its relevance to this paper, an overview of shielded metal arc welding follows. A complete discussion of structural welding is presented by Lancaster [3] and is provided here for further reference.

Currently, the most widely used manual welding process is shielded metal arc welding (SMAW). Undoubtedly, its versatility including the ability to be used in all positions, in confined spaces, and for a wide range of welding applications has contributed to its popularity and widespread use in industry [3].

As one of the fusion welding processes, SMAW produces a fusion weld between the base and filler metals. That is, a weld produced by heating both the base and filler metals to a molten state and allowing them to coalesce and solidify into one piece. In SMAW, the heat source is an electric arc formed between the base metal and a consumable electrode [10]. As the name implies, the metal electrode is consumed during the process to provide the required filler metal. In Figure 2, a schematic illustrating the shielded metal arc welding process is shown.

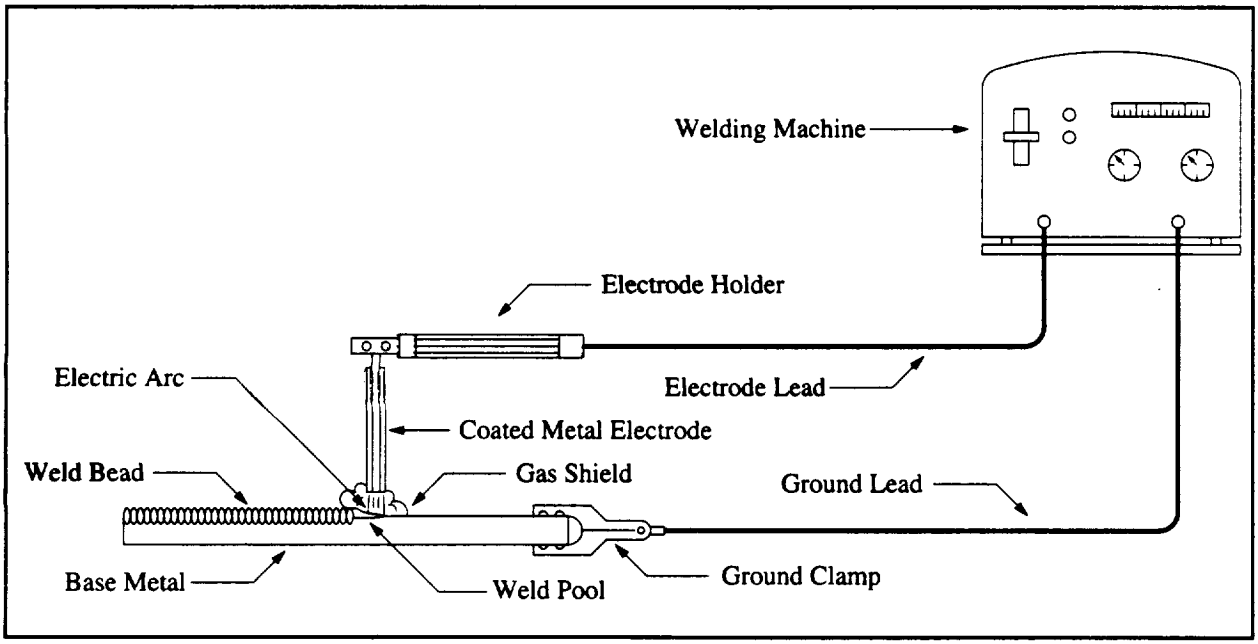

Figure 2. Shielded Metal Arc Welding (SMAW) [10]

It should be emphasized that the flux coating on the electrode plays a pivotal role in SMAW. Most notably, as the electrode is consumed (specifically its flux coating), a blanket of gas is produced that shields the weld from atmospheric contamination [10]. Shielding is absolutely essential given that molten metal readily combines with oxygen, nitrogen, and hydrogen in the atmosphere, and as a consequence can weaken or damage the desired weld properties [10]. In Figure 3, a close-up view of the shielded metal arc welding process is shown including the shielding gas cloud.

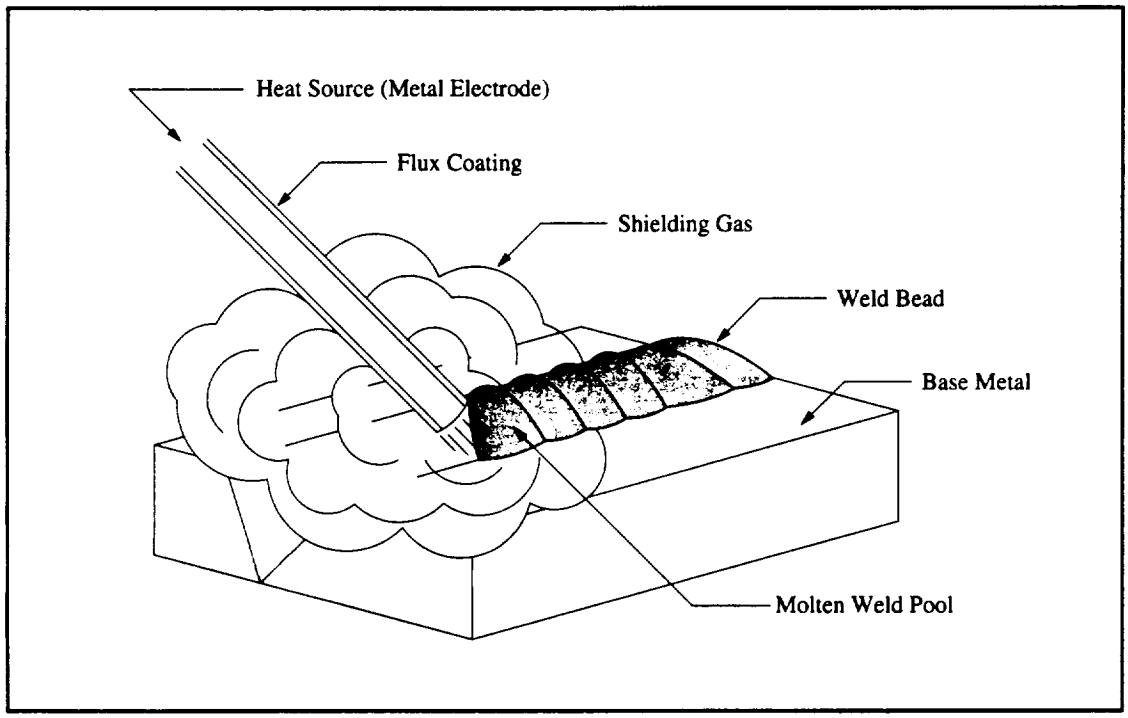

Figure 3. Fusion Welding: Shielded Metal Arc Welding (SMAW) [10]

Lastly, it should be noted that besides producing the gas shield, the flux coating on the electrode is also responsible for generating the arc flow, ensuring directional metal transfer, stabilizing the arc, and promoting a favorable weld chemistry [3]. The interested reader is referred to Lancaster [3] for a more in depth discussion on this subject.

1.2 Previous Work on Structural Optimization

The development of structural optimization, as an engineering discipline, can be traced back to the eighteenth century [11]. However, not until recently, in particular the last forty years, has the application of numerical optimization techniques in structural design been feasibly practical [1]. Most notably in this regard, was the application of nonlinear programming techniques to the design of elastic structures pioneered by Schmit in 1960 [1]. Since then extensive research has been undertaken in the application of structural optimization to real life design problems including, for example, turbine rotors, engine bearing caps, and cooling towers [1]. Vanderplaats [1] and Haftka et al. [11] provide an exhaustive listing of technical papers in reference to this topic and these authors are mentioned here for further reference.

Undoubtedly, the advent of structural optimization as a plausible, real life design tool would not have been made possible if the mathematical complexities associated with it had not been addressed. In particular, the development of the finite element method and its subsequent implementation to the digital computer has been instrumental in this regard. More recently, the availability of low cost high performance computing power, in conjunction with the rapid improvements in the algorithms used for design optimization, have furthermore contributed to the development of structural optimization as a real life design tool [12].

In closing, it should be noted that several structural optimization methods have been developed over the years. They include:

- *The Classical Method*: in the context of this paper (i) sequential unconstrained minimization techniques (SUMT), specifically, the linear extended interior penalty function method (Vanderplaats [1]); (ii) nonlinear goal programming (NLGP) using Powell's conjugate directions method (Vanderplaats [1] and El-Sayed et al. [2]).

- *The Optimality Criteria Method* (Rozvany [12]).

- *The Homogenization Method* (Bendsøe [12]).

1.3 Scope

The primary objective of this work is to develop a reliability based multi-objective design tool. As a test bed, both nonlinear single and multi-objective constrained optimization techniques were applied to the design of a pressure vessel cover plate. In particular, this involved sequential unconstrained minimization techniques, specifically, the linear extended interior penalty function method and nonlinear goal programming based on Powell's conjugate directions method. Optimization criteria included structural weight, load induced stress and deflection, and mechanical reliability. The following is a brief summary of each chapter:

- **Chapter 2** describes the design criteria selected, notably static linear strength, static linear stiffness, and reliability.

- **Chapter 3** presents a discussion on modeling and simulation. In particular, topics of interest include service conditions, FEA, regression analysis, and nonlinear single and multi-objective constrained optimization.

- **Chapter 4** details the finite element modeling of the preselected cover plate including the predicted stress and deflection response.

- **Chapter 5** presents the regression analysis of the FEA data. Highlights include the computation of the stress and deflection functions necessary for numerical optimization.

- **Chapter 6** details the numerical optimization of the preselected cover plate. Highlights include nonlinear single and multi-objective optimization test cases based on: (i) the linear extended interior penalty function method algorithm; and (ii) Powell's conjugate directions method algorithm.

- **Chapter 7** presents conclusions on work completed.

CHAPTER II. DESIGN CRITERIA

Pressure vessels are subject to a wide range of service as well as environmental loading conditions. As defined per the ASME Boiler and Pressure Vessel Code [9] they include:

- internal or external pressure
- weight of vessel and contents
- static reactions from attached equipment, lining, supports
- cyclic and dynamic reactions due to pressure or thermal variations
- impact loading due to fluid shock
- temperature gradients and differential thermal expansion
- wind and seismic forces

Since each one of these loading conditions may constitute a possible mode of failure, the appropriate loading condition pertinent to the desired design must be identified. In the case of a pressure vessel cover plate, and hence in terms of this paper, an internal pressure loading condition was selected for simulation given its prevalence in real life applications. Associated with this loading condition, a set of core/primary design criteria were likewise selected. In particular, they included *static linear strength, static linear stiffness, and reliability.* A brief discussion in reference to these preselected design criteria is presented in the proceeding sections.

2.1 Static Linear Strength

The concept of the static linear strength design criteria is based on the simple premise that the load induced stress at the critical location in the cover plate should be less than or equal to a maximum **allowable/permissible** stress. That is,

$$\sigma \leq \sigma_{max} \tag{2-1}$$

Normalizing yields,

$$\frac{\sigma}{\sigma_{max}} - 1 \leq 0 \tag{2-2}$$

It should be noted that the ASME Boiler and Pressure Vessel Code Section VIII Division 1 provides for a maximum allowable stress of one-quarter the ultimate tensile strength [3].

2.2 Static Linear Stiffness

Similarly, the static linear stiffness design criteria is based on the premise that the load induced deflection at the critical location in the cover plate should be less than or equal to a maximum allowable deflection. That is,

$$z \leq z_{max} \tag{2-3}$$

Normalizing yields,

$$\frac{z}{z_{max}} - 1 \leq 0 \tag{2-4}$$

The maximum allowable deflection is user defined and is selected based on engineering judgment and/or customer specifications.

2.3 Reliability

The reliability design criteria is based on the theory of probability and statistics. In particular, reliability, as referred to in this project, is defined as the probability that the strength exceeds the load induced stress at the critical location in the cover plate [13]. Both strength and stress are observed to be random variables having a normal distribution according to the Central Limit Theorem of Statistics, and are characterized by a mean and a standard deviation [14]. That is,

$$S \sim N(\mu_s, \hat{\sigma}_s) \quad \text{and} \quad \sigma \sim N(\mu_\sigma, \hat{\sigma}_\sigma) \tag{2-5}$$

The so-called coupling equation relates reliability, through the standard normal variate z, to the statistical parameters of the normally distributed strength and stress [13]. That is,

$$z = -\frac{\mu_s - \mu_\sigma}{\left(\hat{\sigma}_s^2 + \hat{\sigma}_\sigma^2\right)^{1/2}} \tag{2-6}$$

Based on the value of z in conjunction with the standard normal distribution curve, the associated reliability is determined as shown in Figure 4.

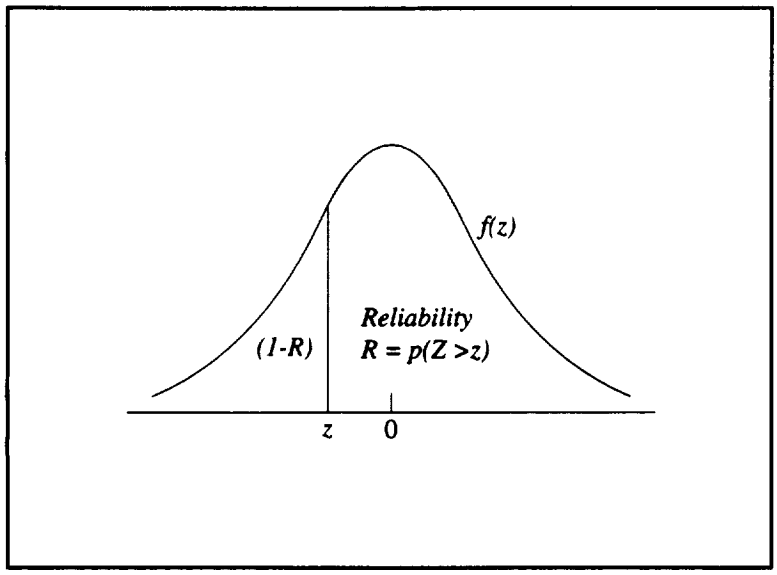

Figure 4. Cumulative Distribution: Standard Normal (Gaussian)

Specifically, it can be shown that [13]

$$R = \int_z^{\infty} \frac{1}{\sqrt{2\pi}} \exp\left(-\frac{u^2}{2}\right) du \qquad (2\text{-}7)$$

Numerical computation of the observed reliability is a fairly simple task once the statistical parameters of the normally distributed strength and stress are known. Based on the concepts inherent in Figure 4 in conjunction with Eq. (2-7), one such approach is shown by the algorithm of Figure 5. In this case

$$I = \int_0^{|z|} \frac{1}{\sqrt{2\pi}} \exp\left(-\frac{u^2}{2}\right) du \qquad (2\text{-}8)$$

Simpson's Rule or trapezoidal approximation can be employed to undertake the necessary numerical integration.

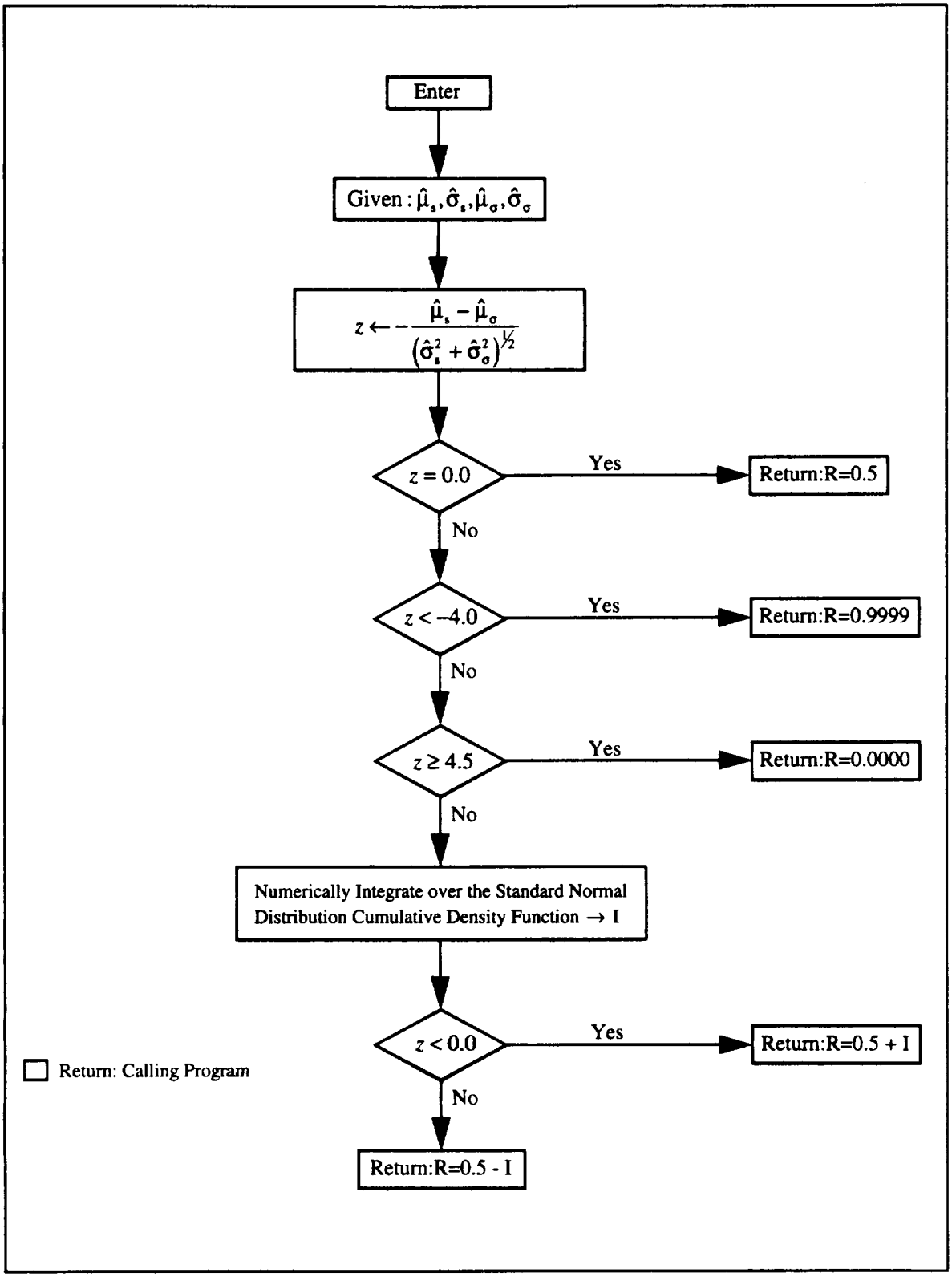

Figure 5. Reliability Algorithm

Lastly, it should be noted that the observed reliability per its definition is consequently a function of the strength and stress statistics. As a result, the reliability design criteria imposes the requirement that the observed reliability be equal to or greater than a target reliability. That is,

$$R \geq R_o \tag{2-9}$$

where R_o is the target and $R(\sigma, S)$ is the observed reliability. Normalizing and inverting the inequality yields,

$$1 - \frac{R}{R_o} \leq 0 \tag{2-10}$$

The target reliability is user defined and is selected based on engineering judgment and/or customer specifications.

CHAPTER III. MODELING AND SIMULATION

The development of a reliability based multi-objective design tool involved the use of both nonlinear single and multi-objective constrained optimization techniques as applied to the design of a pressure vessel cover plate. As a consequence, the geometry and dimensions of the proposed design had to be selected. Likewise, service conditions had to be specified. In addition, the analytical tools necessary to undertake the numerical optimization had to be finalized. Lastly, the nonlinear single and multi-objective optimization design problems had to be formulated. In the proceeding sections an overview of this process is presented.

3.1 Geometry and Service Conditions

In Figures 6 and 7 the geometry and dimensions of the design selected for optimization are shown. In addition, for simulation purposes the following service conditions were adopted:

- a cover plate made of SA-515-70 grade carbon steel with its edges securely fixed (welded seal: SMAW)
- a maximum allowable stress per ASME Code [9]: $\sigma_{max} = \frac{S_{ut}}{4} = 120$ MPa
- a maximum allowable deflection: $z_{max} = 0.1$ mm
- a target reliability: $R_o = 0.999$
- a target structural weight: $W_o = 3.50$ kg
- an inside diameter: $D = 200$ mm
- a maximum uniformly distributed internal design pressure: $P_{max} = 4.2$ MPa

3.2 Stress and Deflection Response

The finite element method in conjunction with regression analysis were selected in order to recover the stress and deflection response necessary for numerical optimization. Specifically,

- Finite Element Analysis: stress and deflection response (ALGOR FEA Software Package)
- Regression Analysis: stress and deflection functions (MINITAB Statistical Software Package)

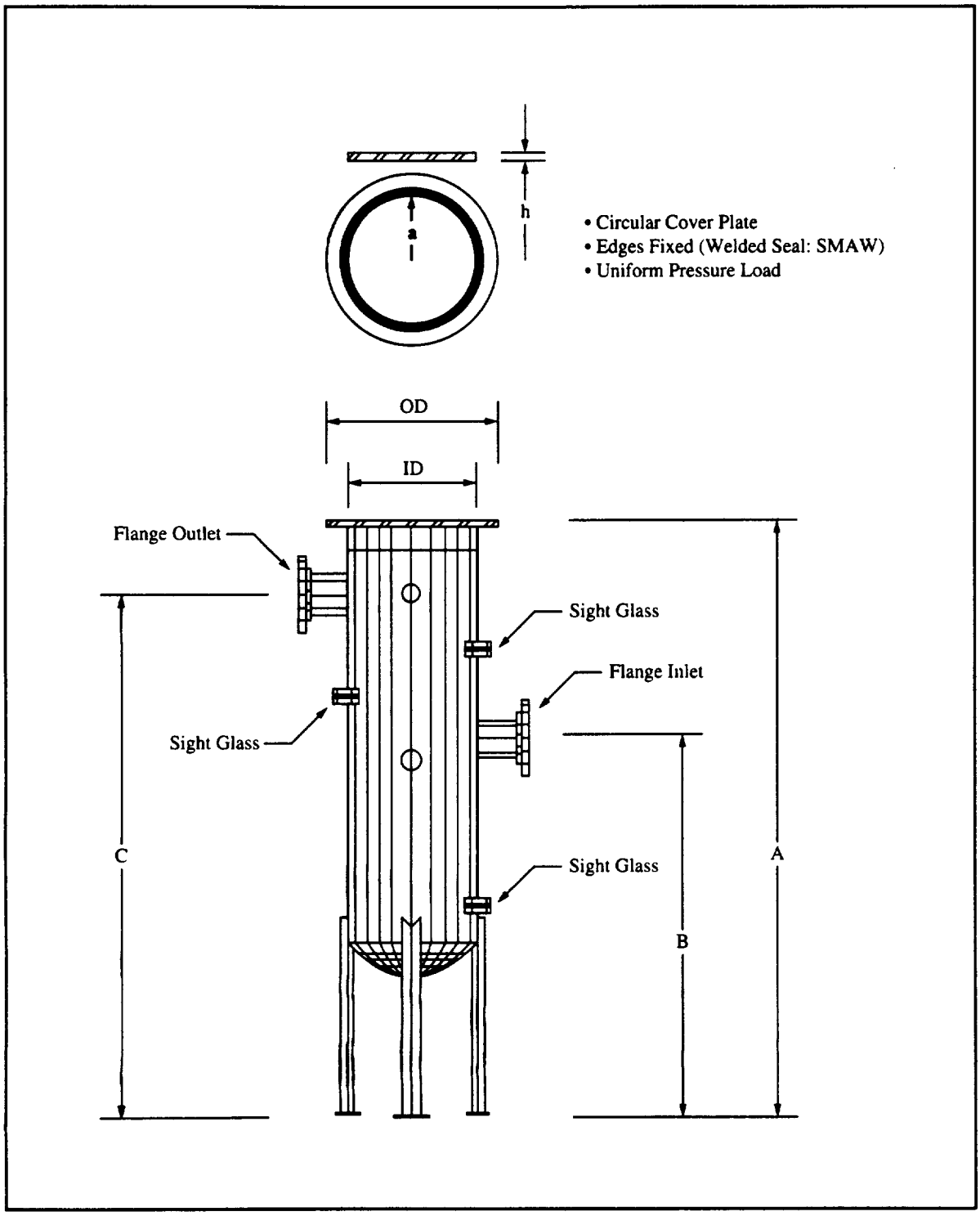

Figure 6. Schematic: Pressure Vessel & Cover Plate

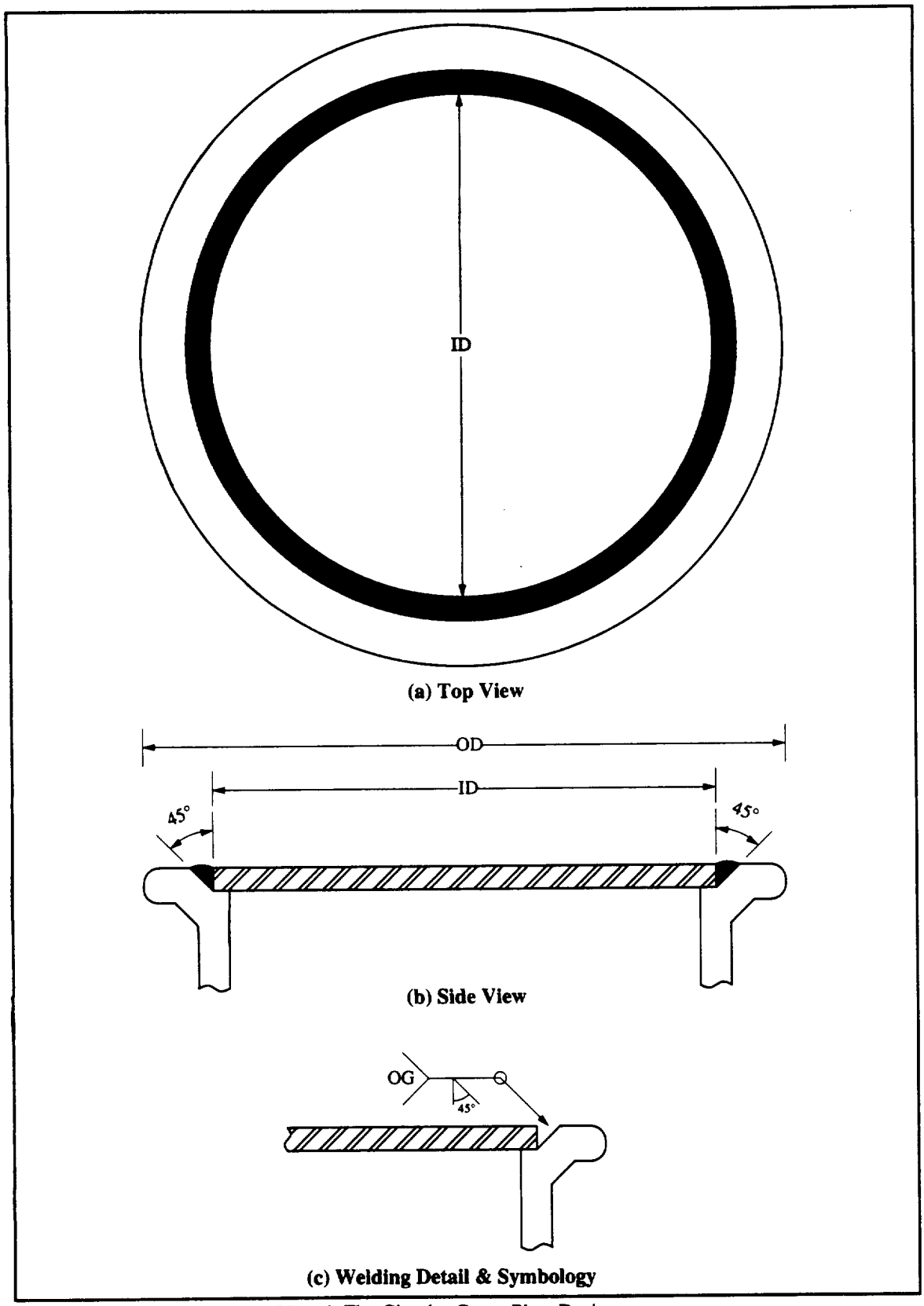

Figure 7. Cylindrical Pressure Vessel: Flat Circular Cover Plate Design

3.3 Nonlinear Constrained Optimization Formulation

Both nonlinear single and multi-objective constrained optimization problems were selected in order to aid in the development of the reliability based multi-objective design tool. In particular, this involved sequential unconstrained minimization techniques (SUMT), specifically, the linear extended interior penalty function method and nonlinear goal programming (NLGP) based on Powell's conjugate directions method. Optimization criteria included structural weight, load induced stress and deflection, and mechanical reliability. The proceeding sections provide a preview of the complete optimization process presented in Chapter VI.

SUMT - Nonlinear Single Objective Constrained Optimization

A nonlinear single objective constrained optimization design problem was selected in order to address two main objectives: (1) ensure predicted optimum design was within ASME Code standards and (2) assess how the variability in the strength characteristics of the cover plate affected the predicted optimum. In particular, based upon the required service conditions in conjunction with the preselected design criteria, the single objective design problem focused on minimizing the structural weight of the cover plate, as a function of its thickness, subject to constraints on stress, deflection, and reliability. That is, find the design variable, h, that would

Minimize: $W(h) = \rho A h$ Objective Function

Subject to:

$$g_1(h) = \frac{\sigma}{\sigma_{max}} - 1 \leq 0$$

$$g_2(h) = \frac{z}{z_{max}} - 1 \leq 0 \qquad \text{Inequality Constraints}$$

$$g_3(h) = 1 - \frac{R}{R_o} \leq 0$$

where

- $\sigma = \sigma(h)$ = FEA/Regression Analysis
- $z = z(h)$ = FEA/Regression Analysis
- $R = R(h) = R(\sigma, S)$: see algorithm of Figure 5

SUMT - Nonlinear Multi-Objective Constrained Optimization

Consequently, a nonlinear multi-objective constrained optimization design problem was selected in order to assess how the selection of weighting factors, in reference to conflicting and multiple objectives, affected the predicted optimum design. In particular, the multi-objective design problem focused on minimizing the structural weight, load induced stress and deflection, and maximizing the reliability of the preselected cover plate, as a function of its thickness, subject to constraints on stress, deflection, and reliability. That is, find the design variable, h, that would

Minimize: $$F(h) = \left\{ w_1 \frac{W(h)}{W_i(h)} + w_2 \frac{\sigma(h)}{\sigma_i(h)} + w_3 \frac{z(h)}{z_i(h)} - w_4 \frac{R(h)}{R_i(h)} \right\}$$ Composite Objective Function

Subject to:

$$g_1(h) = \frac{\sigma}{\sigma_{max}} - 1 \leq 0$$

$$g_2(h) = \frac{z}{z_{max}} - 1 \leq 0$$ Inequality Constraints

$$g_3(h) = 1 - \frac{R}{R_o} \leq 0$$

where

- w_n (for n = 1, 2, 3, 4) are the weighting factors
- $W(h) = \rho A h$
- $\sigma = \sigma(h)$ = FEA/Regression Analysis
- $z = z(h)$ = FEA/Regression Analysis
- $R = R(h) = R(\sigma, S)$: see algorithm of Figure 5
- **ith subscript indicates function** value at initial value of design variable

NLGP - Nonlinear Multi-Objective Constrained Optimization

Lastly, a nonlinear multi-objective constrained optimization problem, based on goal programming, was selected in order to assess how the selection of a preemptive priority system, in reference to conflicting and multiple objectives, affected the predicted optimum design. In particular, the multi-objective design problem focused on minimizing the sum of deviational variables, in a preemptive priority system, subject to constraints on structural weight, stress, deflection, and reliability. That is, find the design variable, h, that would

$$\text{Minimize:} \quad \mathbf{z} = \begin{Bmatrix} \text{weighted deviations of Priority 1} \\ \text{weighted deviations of Priority 2} \\ \cdot \\ \cdot \\ \text{weighted deviations of Priority K} \end{Bmatrix} \qquad \text{Achievement Vector}$$

Subject to:

$$\frac{W}{W_o} - 1 = \text{deviation 1}$$

$$\frac{\sigma}{\sigma_{max}} - 1 = \text{deviation 2}$$

$$\frac{z}{z_{max}} - 1 = \text{deviation 3} \qquad \text{Design Constraints}$$

$$\frac{R}{R_o} - 1 = \text{deviation 4}$$

and side constraints

$$5 \leq h \leq 40$$

where

- $W = W(h) = \rho A h$
- $\sigma = \sigma(h)$ = FEA/Regression Analysis
- $z = z(h)$ = FEA/Regression Analysis
- $R = R(h) = R(\sigma, S)$: see algorithm of Figure 5

CHAPTER IV. FINITE ELEMENT ANALYSIS

In order to recover the stress and deflection response necessary for numerical optimization, both the finite element method in conjunction with regression analysis were employed. In this chapter, the finite element analysis of the cover plate preselected for optimization is presented. In particular, the proceeding sections discuss the applied boundary conditions and loads as well as the test cases that were run.

4.1 Boundary Conditions and Loads

The finite element analysis of the preselected cover plate was undertaken using the Algor finite element software package. Loading conditions required the plate to be subject to a uniformly distributed design pressure along the -z direction having a magnitude of 4.2 MPa. Boundary conditions required that the plate's edges be securely clamped. This meant that nodes along the plate's periphery were restricted so as to experience no translation or rotation. Service conditions also required:

- Stress units: Pa
- Displacement units: m
- Young's Modulus, E = 200 GPa
- Poisson's Ratio, $\nu = 0.29$
- Inside Diameter, D = 0.2 m
- Internal Design Pressure, $P_{max} = 4.2$ MPa
- Material: Isotropic SA-515-70 grade carbon steel

4.2 Test Cases

Eight design test cases were analyzed in terms of both maximum principal stress and predicted deflection. In each case, a 3-D model was generated using 224 three-dimensional plate/shell elements with 210 global nodes. In the proceeding pages the results obtained are presented.

Test Case #1: Cover Plate Thickness, h = 5 mm.

Finite Element Model: 224 plate elements with 210 global nodes.

i) Stress Distribution:

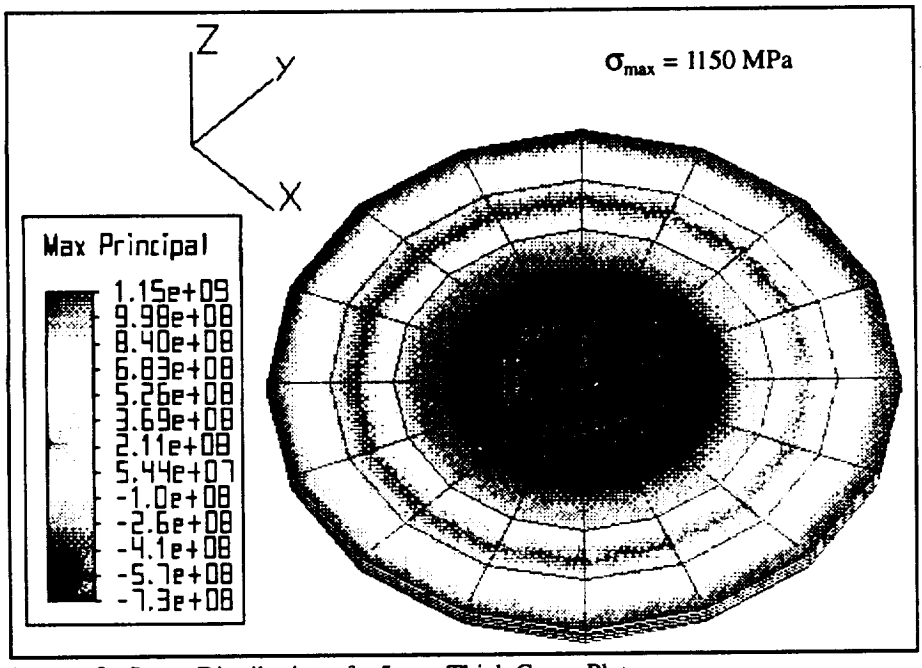

Figure 8. Stress Distribution of a 5 mm Thick Cover Plate

• Note: Consistent with the Theory of Flexure of Plates [15]: (i) Maximum principal stress occurs along the periphery of the cover plate. (ii) Maximum deflection occurs at the center of the cover plate.

ii) Plate Deflection:

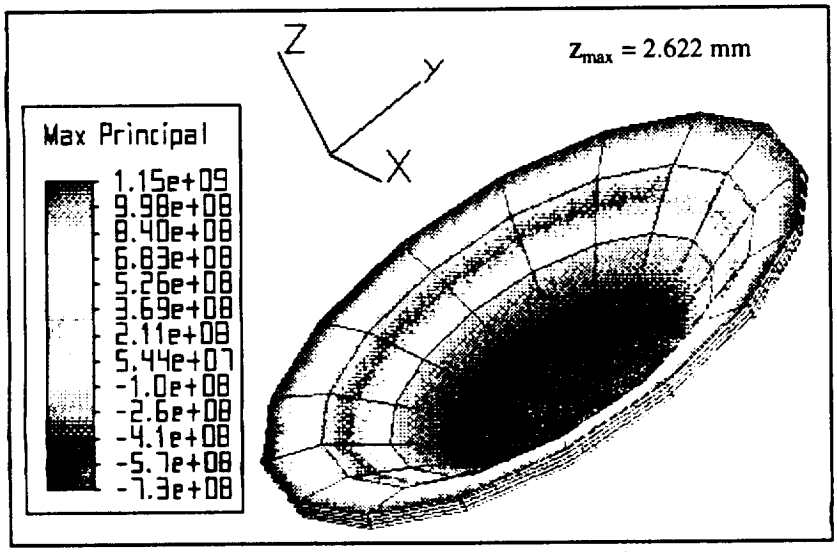

Figure 9. Predicted Deflection of a 5 mm Thick Cover Plate

Test Case #2: Cover Plate Thickness, h = 10 mm.

Finite Element Model: 224 plate elements with 210 global nodes.

i) Stress Distribution:

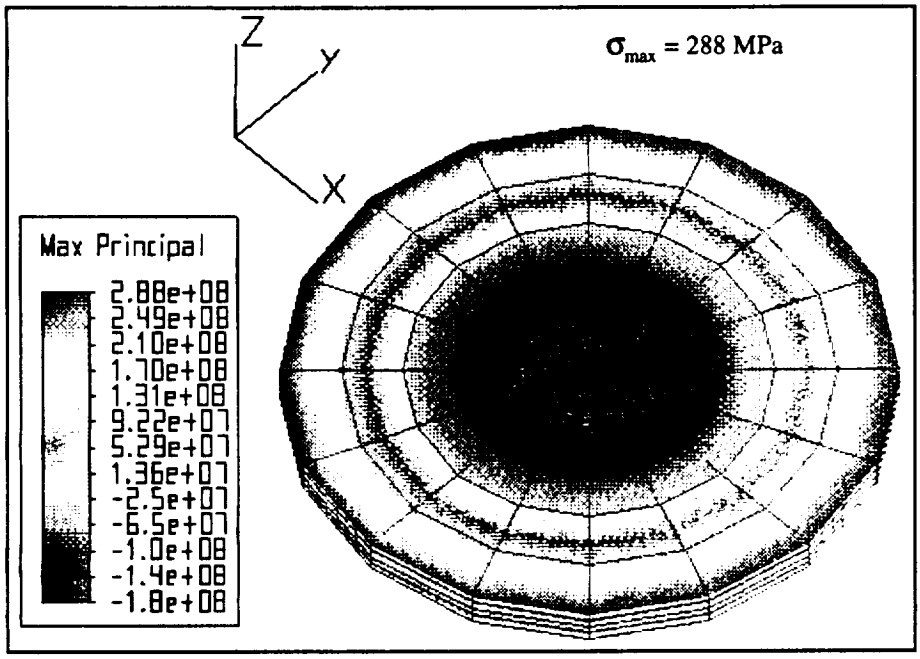

Figure 10. Stress Distribution of a 10 mm Thick Cover Plate

• Note: Consistent with the Theory of Flexure of Plates [15]: (i) Maximum principal stress occurs along the periphery of the cover plate. (ii) Maximum deflection occurs at the center of the cover plate.

ii) Plate Deflection:

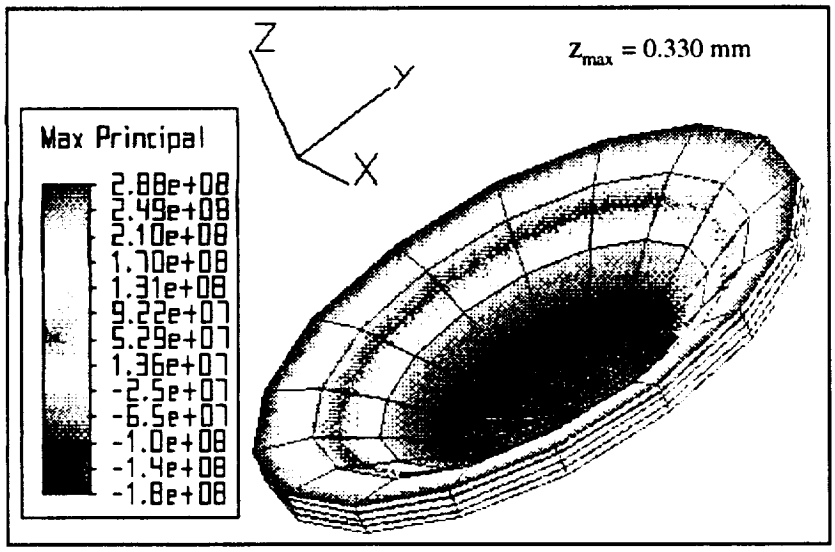

Figure 11. Predicted Deflection of a 10 mm Thick Cover Plate

Test Case #3: Cover Plate Thickness, h = 15 mm.

Finite Element Model: 224 plate elements with 210 global nodes.

i) Stress Distribution:

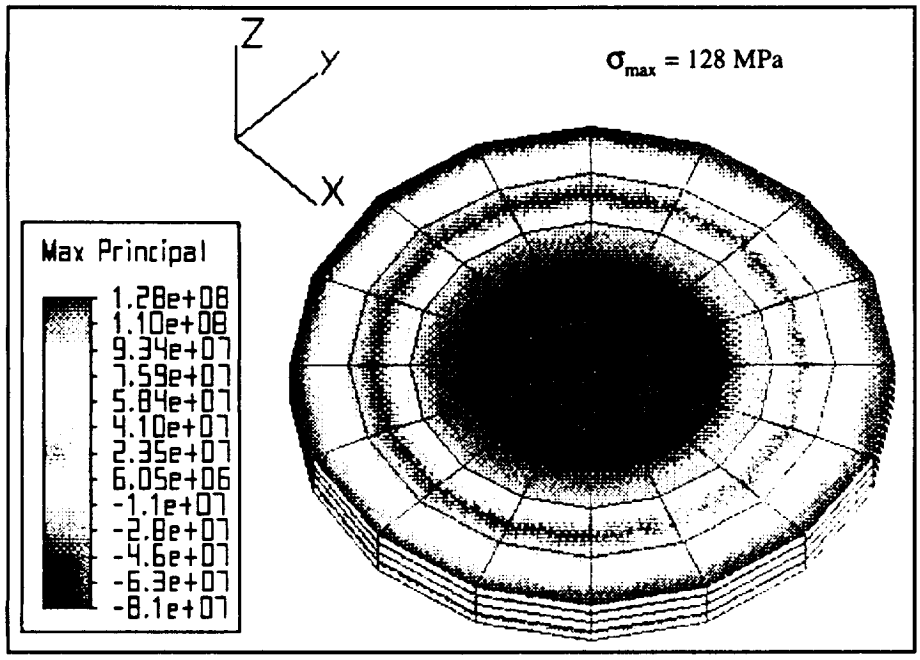

Figure 12. Stress Distribution of a 15 mm Thick Cover Plate

• Note: Consistent with the Theory of Flexure of Plates [15]: (i) Maximum principal stress occurs along the periphery of the cover plate. (ii) Maximum deflection occurs at the center of the cover plate.

ii) Plate Deflection:

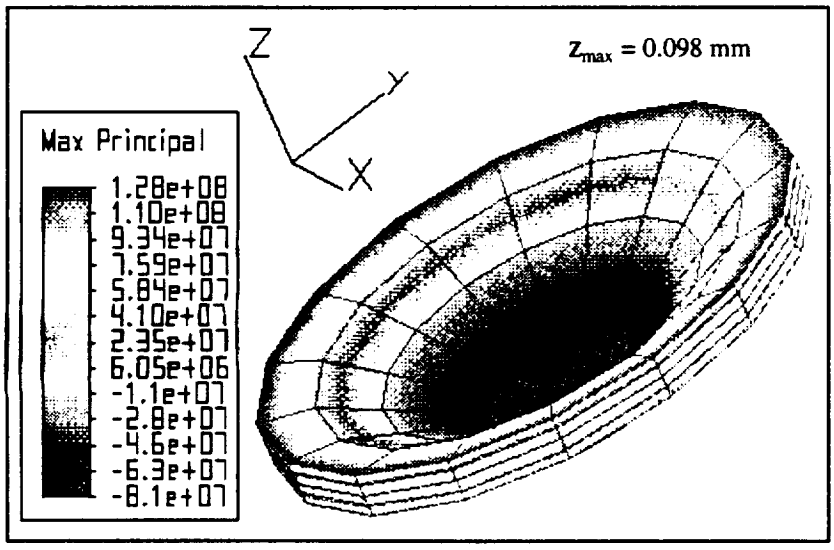

Figure 13. Predicted Deflection of a 15 mm Thick Cover Plate

Test Case #4: Cover Plate Thickness, h = 20 mm.

Finite Element Model: 224 plate elements with 210 global nodes.

i) Stress Distribution:

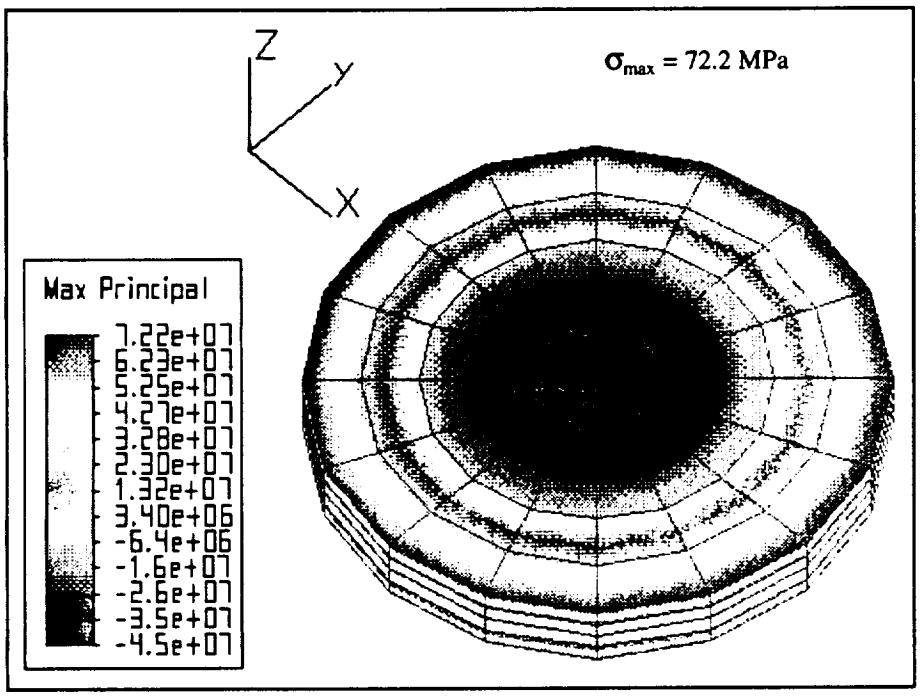

Figure 14. Stress Distribution of a 20 mm Thick Cover Plate

• Note: Consistent with the Theory of Flexure of Plates [15]: (i) Maximum principal stress occurs along the periphery of the cover plate. (ii) Maximum deflection occurs at the center of the cover plate.

ii) Plate Deflection:

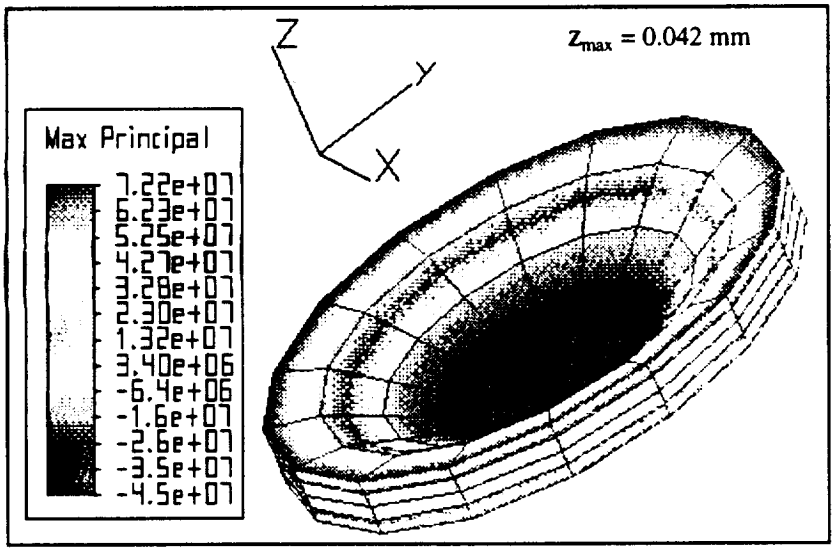

Figure 15. Predicted Deflection of a 20 mm Thick Cover Plate

Test Case #5: Cover Plate Thickness, h = 25 mm.

Finite Element Model: 224 plate elements with 210 global nodes.

i) Stress Distribution:

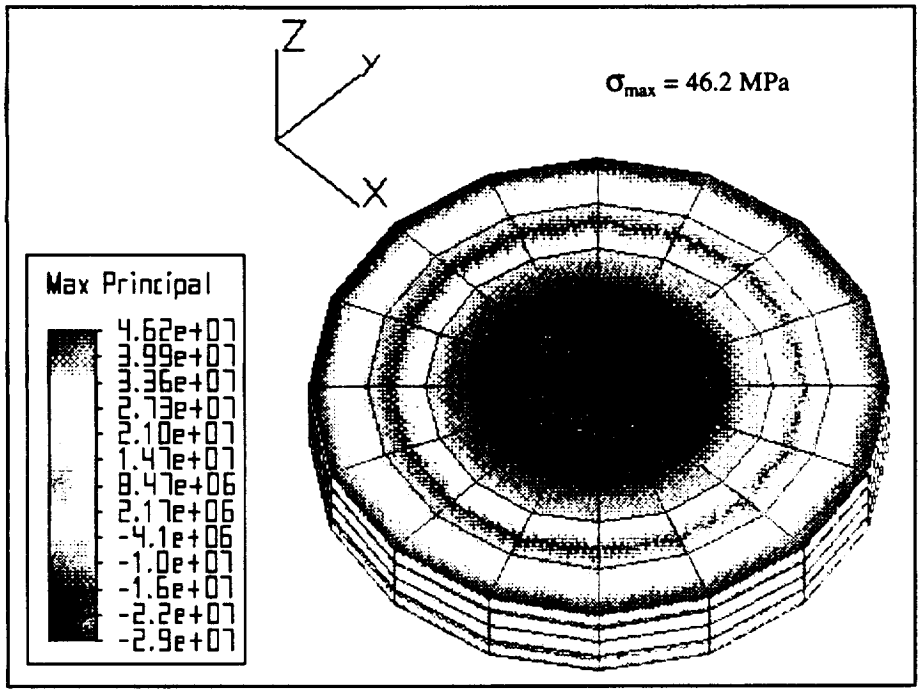

Figure 16. Stress Distribution of a 25 mm Thick Cover Plate

• Note: Consistent with the Theory of Flexure of Plates [15]: (i) Maximum principal stress occurs along the periphery of the cover plate. (ii) Maximum deflection occurs at the center of the cover plate.

ii) Plate Deflection:

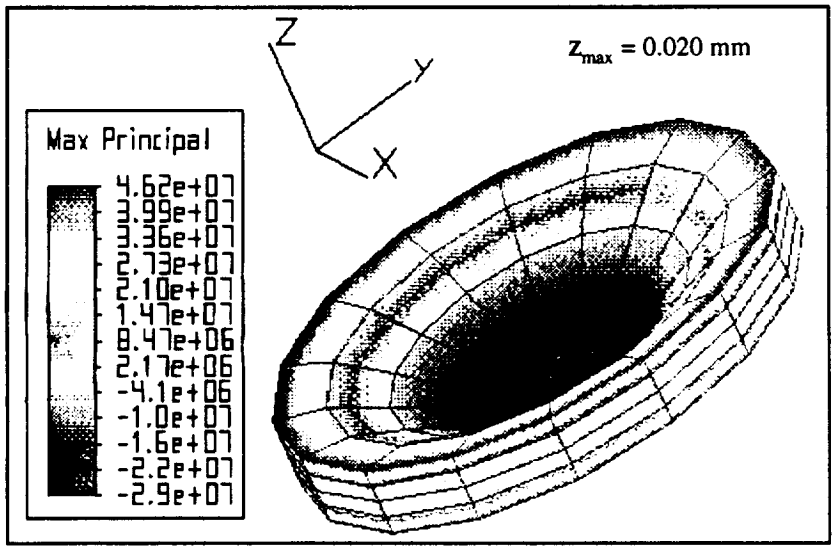

Figure 17 Predicted Deflection of a 25 mm Thick Cover Plate

Test Case #6: Cover Plate Thickness, h = 30 mm.

Finite Element Model: 224 plate elements with 210 global nodes.

i) Stress Distribution:

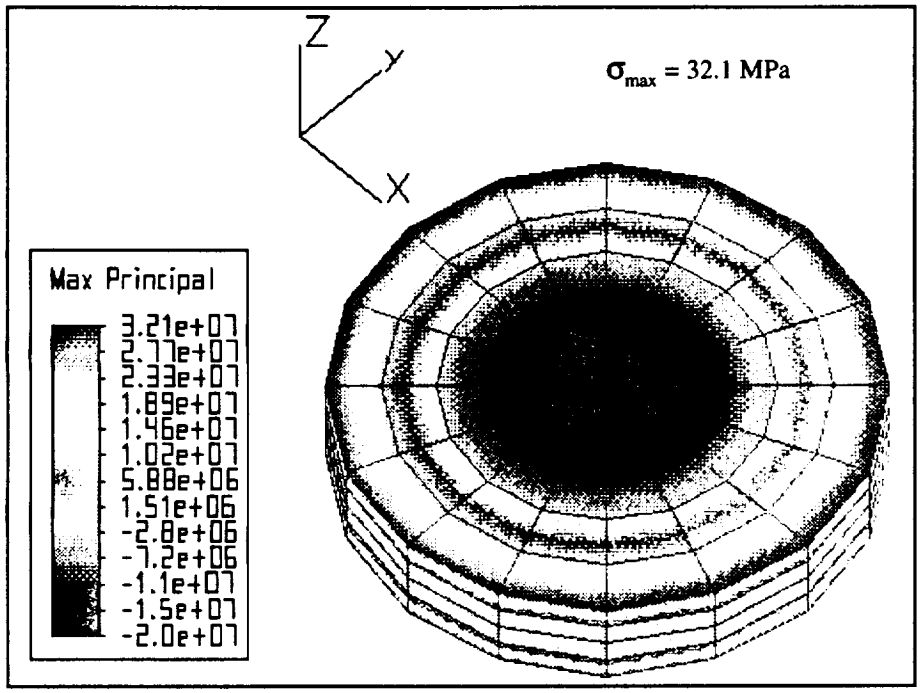

Figure 18. Stress Distribution of a 30 mm Thick Cover Plate

• Note: Consistent with the Theory of Flexure of Plates [15]: (i) Maximum principal stress occurs along the periphery of the cover plate. (ii) Maximum deflection occurs at the center of the cover plate.

ii) Plate Deflection:

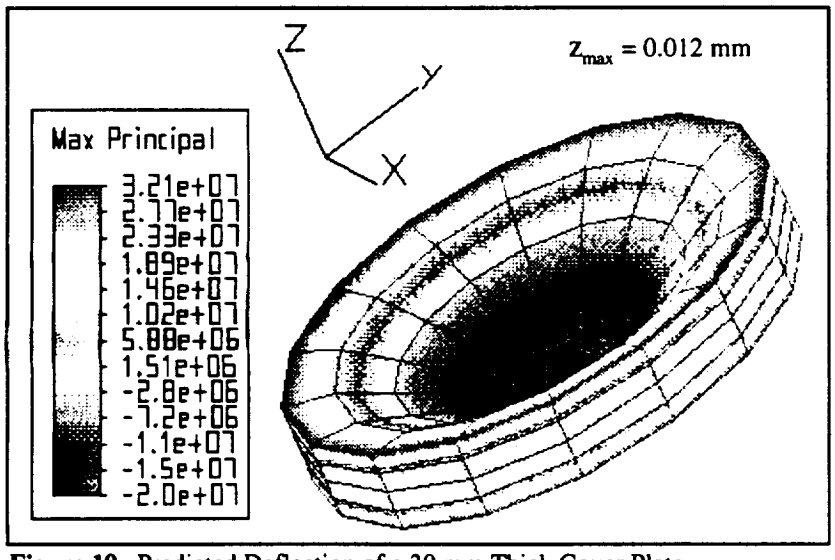

Figure 19. Predicted Deflection of a 30 mm Thick Cover Plate

Test Case #7: Cover Plate Thickness, h = 35 mm.

Finite Element Model: 224 plate elements with 210 global nodes.

i) Stress Distribution:

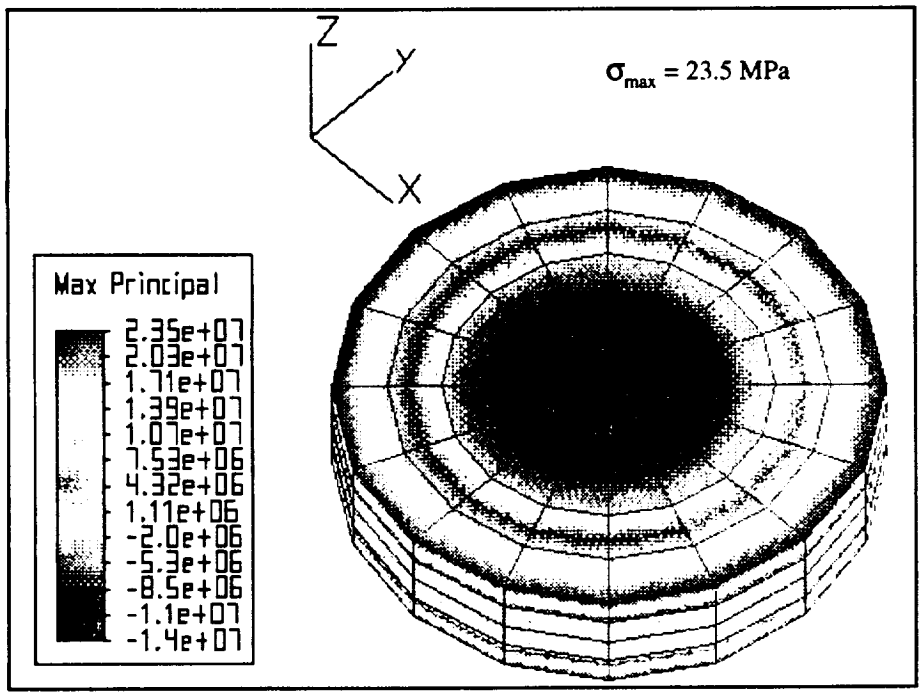

Figure 20. Stress Distribution of a 35 mm Thick Cover Plate

• Note: Consistent with the Theory of Flexure of Plates [15]: (i) Maximum principal stress occurs along the periphery of the cover plate. (ii) Maximum deflection occurs at the center of the cover plate.

ii) Plate Deflection:

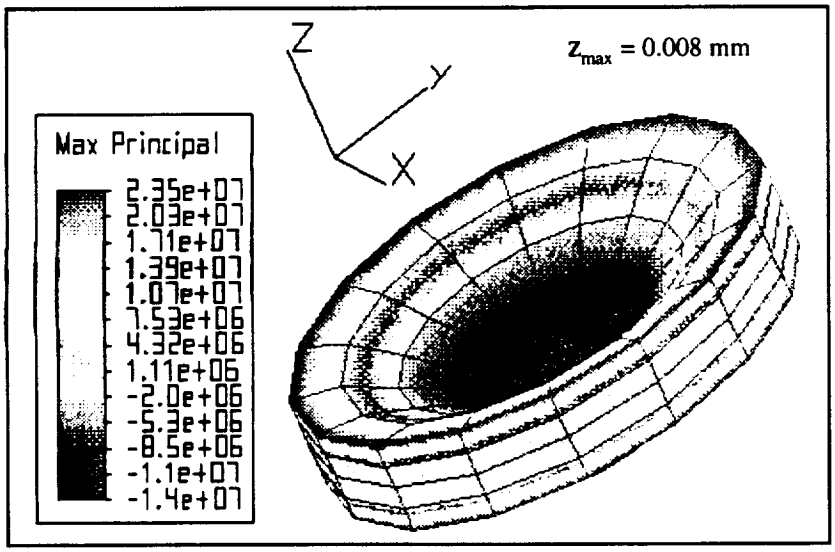

Figure 21. Predicted Deflection of a 35 mm Thick Cover Plate

Test Case #8: Cover Plate Thickness, h = 40 mm.

Finite Element Model: 224 plate elements with 210 global nodes.

i) Stress Distribution:

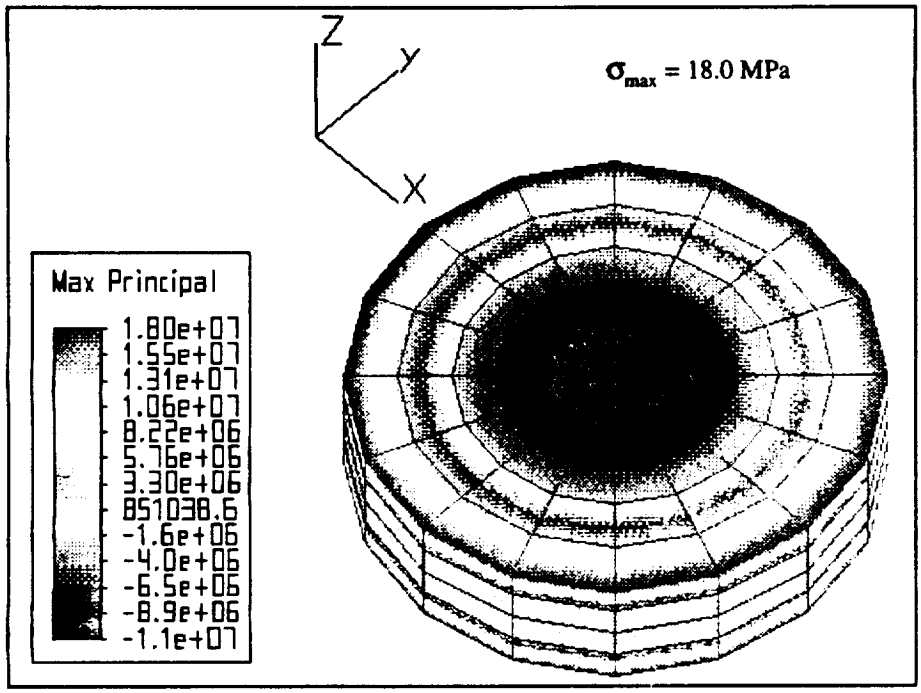

Figure 22. Stress Distribution of a 40 mm Thick Cover Plate

• Note: Consistent with the Theory of Flexure of Plates [15]: (i) Maximum principal stress occurs along the periphery of the cover plate. (ii) Maximum deflection occurs at the center of the cover plate.

ii) Plate Deflection:

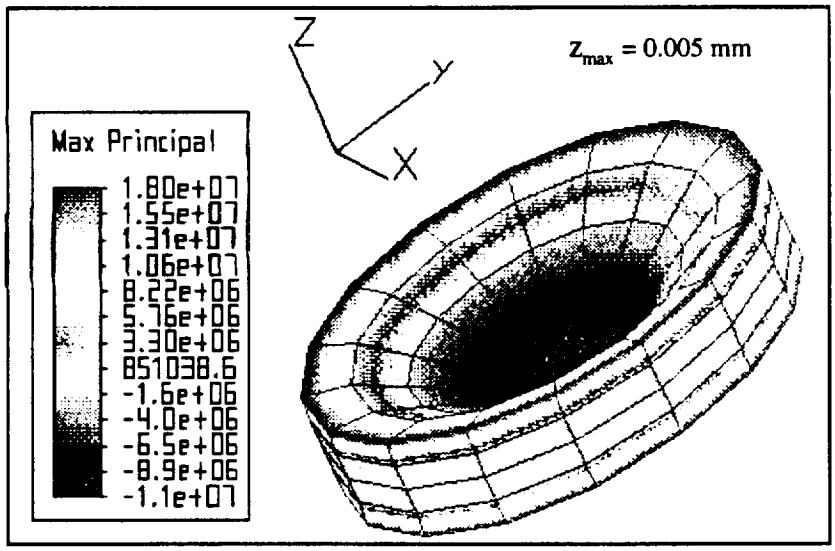

Figure 23. Predicted Deflection of a 40 mm Thick Cover Plate

CHAPTER V. REGRESSION ANALYSIS

This chapter presents the regression analysis associated with the results of the finite element analysis presented in Chapter IV. In particular, the chapter details the computation of the stress and deflection functions necessary for numerical optimization. In Table 1, a summary of the important findings that were obtained during finite element modeling are listed for reference.

Table 1. Maximum Principal Stress and Deflection Data

Test Case #	Thickness h, mm	Maximum Principal Stress σ, MPa	Maximum Deflection z, mm
1	5	1150	2.622
2	10	288	0.330
3	15	128	0.098
4	20	72.2	0.042
5	25	46.2	0.020
6	30	32.1	0.012
7	35	23.5	0.008
8	40	18.0	0.005

In the proceeding sections a comprehensive regression analysis of the data in Table 1 follows including:

- scatter plots of the response and regressor variables
- formulation of the proposed regression model(s)
- parameter estimation in reference to the proposed regression model(s)
- diagnostic tests: model utility and residual analysis

5.1 Scatter Plots

Successful fitting of a regression model requires a careful analysis of the database for the problem under study. As part of this analysis, plotting the variables of interest is an invaluable first step in assessing the relationship between the independent (regressor) and dependent (response) variable(s).

In reference to the data presented in Table 1 and as a consequence of importance for numerical optimization purposes, the key variables of interest included: the thickness (regressor variable)

of the preselected cover plate and the load induced maximum principal stress and deflection (response variables). In Figures 24 and 25 the scattergrams of thickness versus maximum principal stress and thickness versus maximum deflection are shown respectively.

Maximum Principal Stress

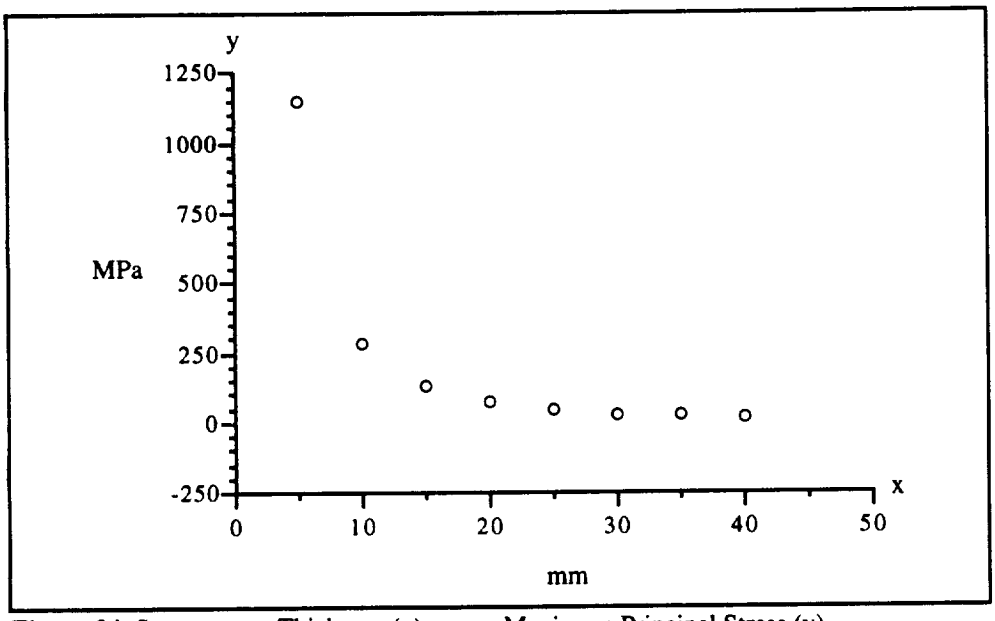

Figure 24. Scattergram: Thickness (x) versus Maximum Principal Stress (y)

Maximum Deflection

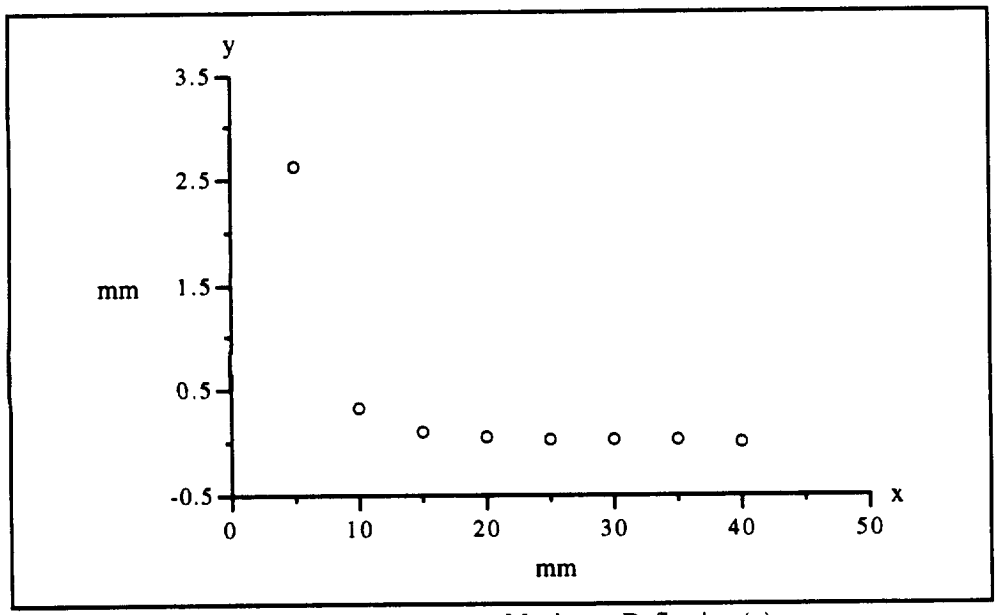

Figure 25. Scattergram: Thickness (x) versus Maximum Deflection (y)

5.2 Proposed Regression Model

Based on the scatter plots of Figures 24 and 25 in conjunction with the Theory of Flexure of Plates [15], a power regression model was proposed for both the maximum principal stress and deflection. In general, the power regression model [14] assumes the form

$$\mu_{Y|x} = \beta_o x^{\beta_1} \quad \text{for } x > 0 \tag{5-1}$$

or

$$y_i = \beta_o x_i^{\beta_1} e_i \quad \text{for } x > 0 \tag{5-2}$$

A logarithmic transformation is used to linearize this model as follows:

$$\ln y_i = \ln \beta_o x_i^{\beta_1} e_i \tag{5-3}$$

or

$$\ln y_i = \ln \beta_o + \beta_1 \ln x_i + \ln e_i \tag{5-4}$$

The new linear model becomes

$$y_i^* = \beta_o^* + \beta_1^* x_i^* + e_i^* \tag{5-5}$$

where $y_i^* = \ln y_i$, $\beta_o^* = \ln \beta_o$, $\beta_1^* = \beta_1$, $x_i^* = \ln x_i$ and $e_i^* = \ln e_i$. Parameter estimates are $\hat{\beta}_1 = \hat{\beta}_1^*$ and $\hat{\beta}_o = e^{\beta_o^*}$.

5.3 Parameter Estimation

Based on the proposed power regression model of Eq. (5-2), parameter estimation required a logarithmic transformation of the database, parameter transformation, formulation of the power regression equation, and finally a check on model utility. In the proceeding sections the results obtained for both the maximum principal stress and deflection models are presented.

Maximum Principal Stress

Consistent with Eq. (5-3) the required logarithmic transformation of the database is shown in Table 2.

Table 2. Maximum Principal Stress: Logarithmic Transformation

Test Case #	Thickness h, mm	Regressor Transform ln (h)	Maximum Principal Stress σ, MPa	Response Transform ln (σ)
1	5	1.60944	1150	7.04752
2	10	2.30258	288	5.66296
3	15	2.70805	128	4.85203
4	20	2.99573	72.2	4.27944
5	25	3.21888	46.2	3.83298
6	30	3.40120	32.1	3.46886
7	35	3.55535	23.5	3.15700
8	40	3.68888	18.0	2.89037

Using the MINITAB statistical software package, the linear regression analysis of the data in Table 2 was undertaken. In particular, the regression analysis was based on x = ln(h) and y = ln (σ). The MINITAB output follows.

```
Regression Analysis

The regression equation is
y = 10.3 - 2.00 x

Predictor       Coef        Stdev    t-ratio        p
Constant     10.2652       0.0027    3792.62    0.000
x           -1.99873      0.00090   -2221.18    0.000

s = 0.001675    R-sq = 100.0%    R-sq(adj) = 100.0%
```

a. Parameter Transformation

Based on Eq. (5-5) the appropriate parameter transformation yields

$$\hat{\beta}_0 = e^{\beta_0^*} = e^{10.2652} = 28716 \quad \text{and} \quad \hat{\beta}_1 = \beta_1^* = -2.0 \qquad (5\text{-}6)$$

b. Power Regression Equation

Substituting the parameter estimates of Eq. (5-6) into Eq. (5-2) yields

$$\sigma = 28716h^{-2.0} \qquad (5\text{-}7)$$

Consistent with the Theory of Flexure of Plates [15], the obtained regression equation confirms that the maximum principal stress is inversely proportional to the square of the cover plate's thickness.

c. Model Utility

Based that the null hypothesis H_o: $\beta_1^* = 0$ can be rejected with $p = 0.000$, the regression is significant. That is, the model is useful in predicting the maximum principal stress based on the cover plate's thickness. The R^2 statistic furthermore suggests that 100% of the total variation in the maximum principal stress is indeed explained by the plate's thickness. Figure 26 shows the fitted model and suggests a good fit.

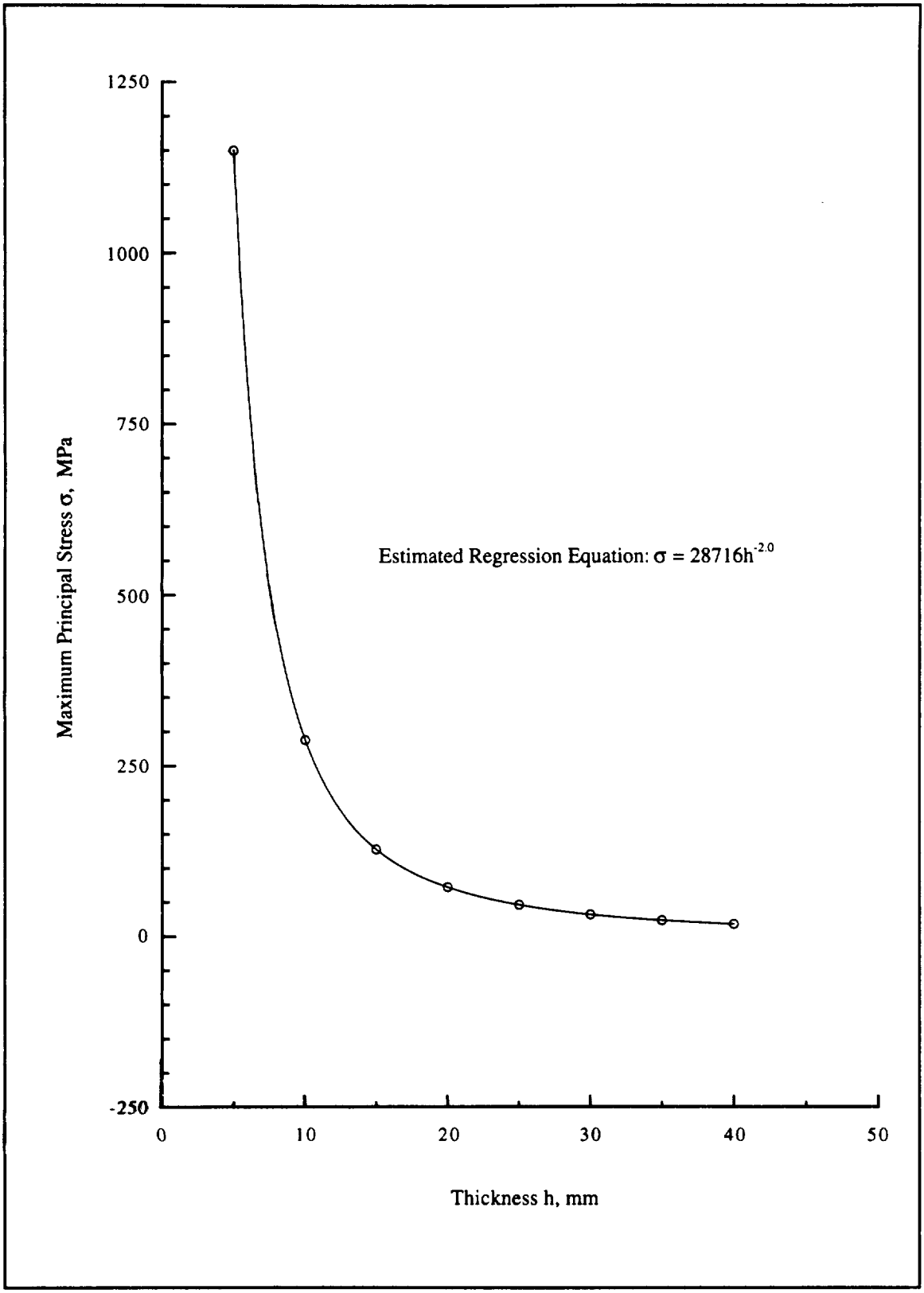

Figure 26. Maximum Principal Stress as a Function of Plate Thickness

Maximum Deflection

Consistent with Eq. (5-3) the required logarithmic transformation of the database is shown in Table 3.

Table 3. Maximum Deflection: Logarithmic Transformation

Test Case #	Thickness h, mm	Regressor Transform ln (h)	Maximum Deflection z, mm	Response Transform ln (z)
1	5	1.60944	2.622	0.96394
2	10	2.30258	0.330	-1.10866
3	15	2.70805	0.098	-2.32279
4	20	2.99573	0.042	-3.17009
5	25	3.21888	0.020	-3.91202
6	30	3.40120	0.012	-4.42285
7	35	3.55535	0.008	-4.82831
8	40	3.68888	0.005	-5.29832

Using MINITAB, the linear regression analysis of the data in Table 3 was undertaken. In particular, the regression analysis was based on x = ln(h) and y = ln (z). The MINITAB output follows.

```
Regression Analysis

The regression equation is
y = 5.80 - 3.00 x

Predictor       Coef        Stdev     t-ratio         p
Constant     5.80418      0.04998      116.14     0.000
x           -3.00393      0.01662     -180.79     0.000

s = 0.03092     R-sq = 100.0%     R-sq(adj) = 100.0%
```

a. Parameter Transformation

Based on Eq. (5-5) the appropriate parameter transformation yields

$$\hat{\beta}_o = e^{\beta_o^*} = e^{5.80418} = 331.68 \quad \text{and} \quad \hat{\beta}_1 = \beta_1^* = -3.0 \qquad (5\text{-}8)$$

b. Power Regression Equation

Substituting the parameter estimates of Eq. (5-8) into Eq. (5-2) yields

$$z = 331.68h^{-3.0} \qquad (5\text{-}9)$$

Consistent with the Theory of Flexure of Plates [15], the obtained regression equation confirms that the maximum deflection is inversely proportional to the cubic power of the cover plate's thickness.

c. Model Utility

Based that the null hypothesis H_o: $\beta_1^* = 0$ can be rejected with $p = 0.000$, the regression is significant. That is, the model is useful in predicting the maximum deflection based on the cover plate's thickness. The R^2 statistic furthermore suggests that 100% of the total variation in the maximum deflection is indeed explained by the plate's thickness. Figure 27 shows the fitted model and suggests a good fit.

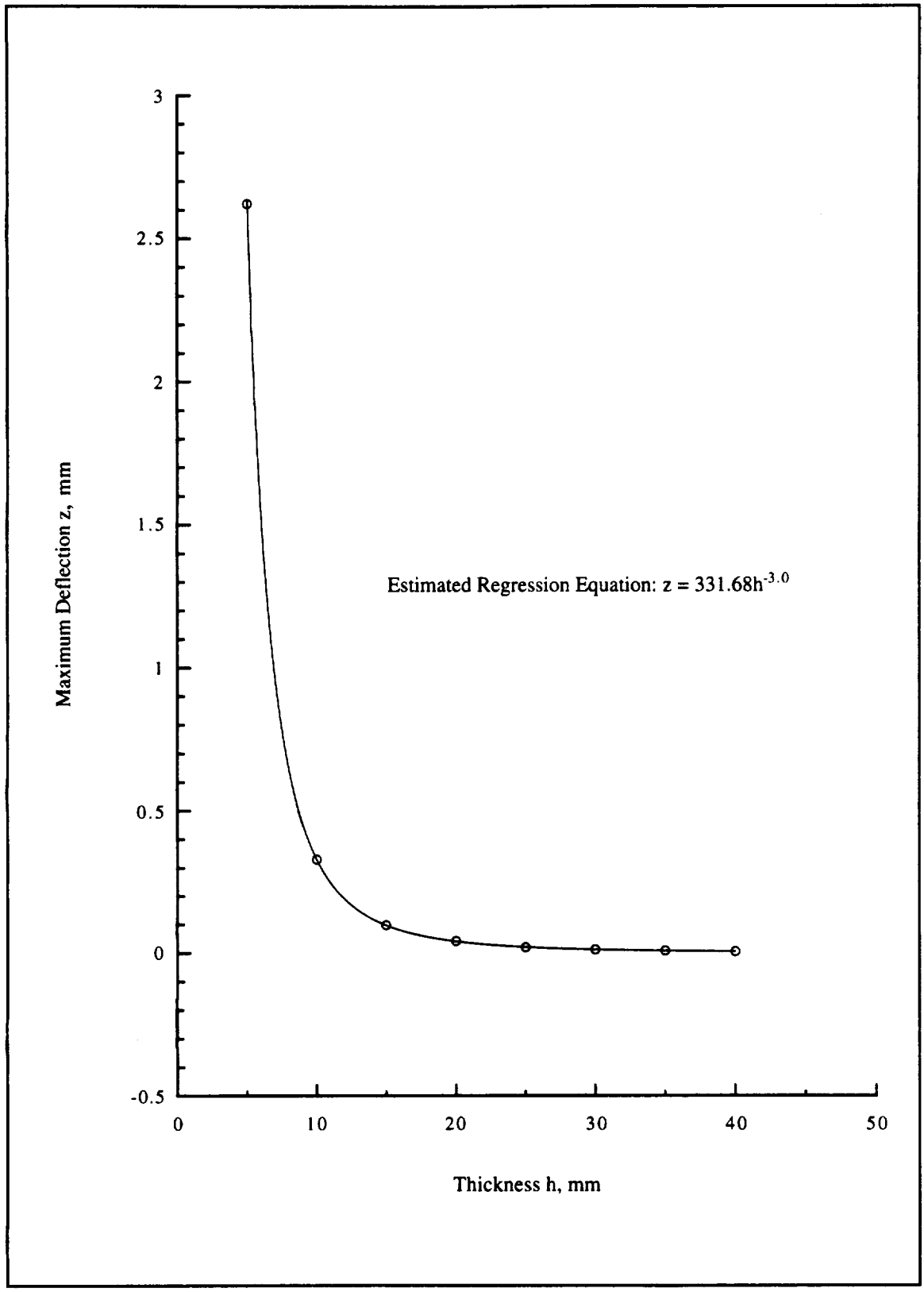

Figure 27. Maximum Deflection as a Function of Plate Thickness

5.4 Residual Analysis

As a final diagnostic test, verifying the validity of the regression models introduced in Sect. 5.3, a residual analysis [14] was conducted. In particular, the basic underlying assumptions of these models were verified. Most notably, this involved verifying that the residuals (i.e. the difference between the observed response and the predicted value) were independent, exhibited a constant variance and were normally distributed random variables with mean 0. Nongraphical as well as graphical techniques were used in the assessment of the validity of these assumptions. In the proceeding sections the residual analysis of both the maximum principal stress and maximum deflection regression models are presented.

Test for Independence

Using the MINITAB statistical software package, the test for independence involved computing the so-called Durbin-Watson statistic. The MINITAB output for both regression models follows.

a. Maximum Principal Stress Regression Model

```
Durbin-Watson statistic = 1.26
```

b. Maximum Deflection Regression Model

```
Durbin-Watson statistic = 2.60
```

- **Conclusion**

  Based on the results of both parts (a) and (b), the null hypothesis of independence H_o can not be rejected at the 1% level [16]. That is, the assumption of independence, in each case, does not appear to be violated.

Homogeneity of Variance

Using MINITAB, a standard residual plot was generated to test for homogeneity of variance. The results obtained for both the maximum principal stress and maximum deflection regression models are shown in Figures 28 and 29 respectively.

a. Maximum Principal Stress Regression Model

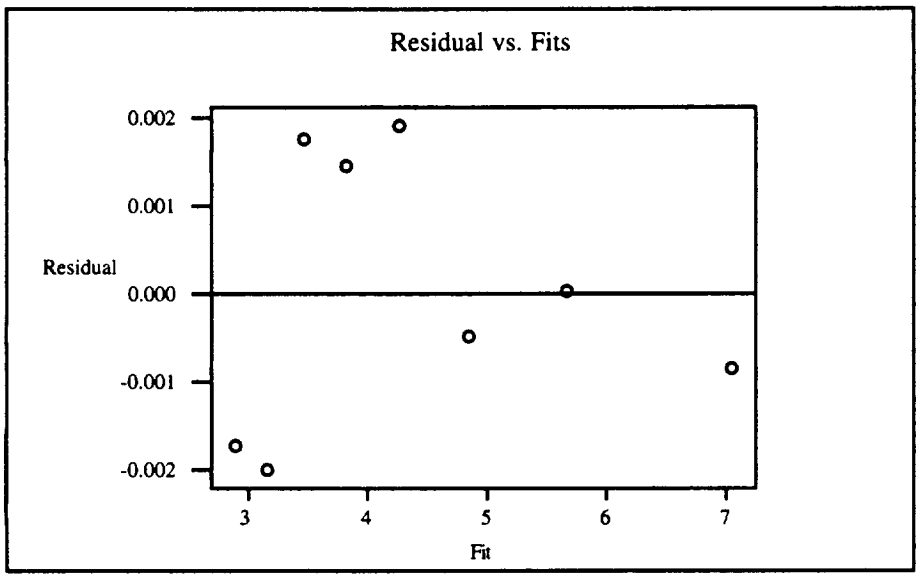

Figure 28. Standard Residual Plot: Maximum Principal Stress

b. Maximum Deflection Regression Model

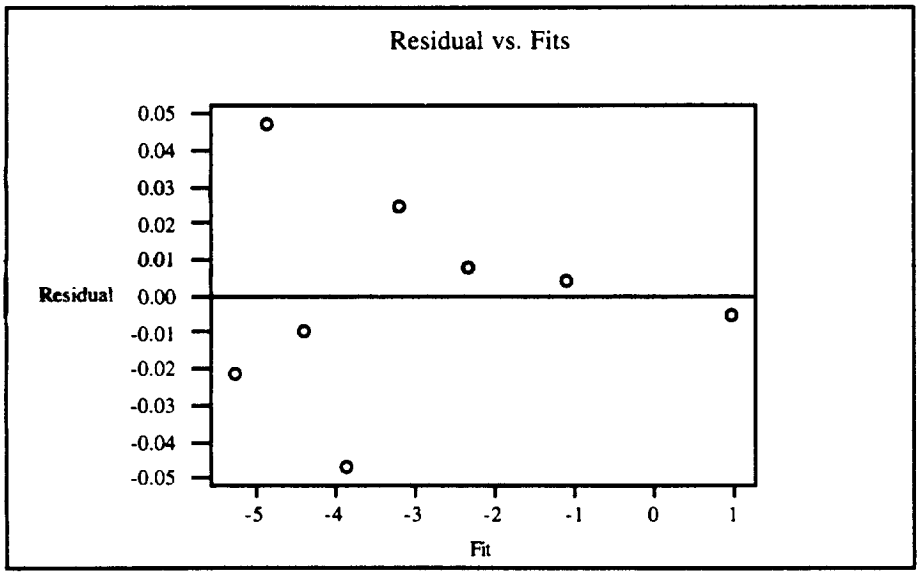

Figure 29. Standard Residual Plot: Maximum Deflection

• **Conclusion**

Given that in both Figures 28 and 29 the residuals are scattered randomly about 0 with a uniform spread, the assumption of common variance, in both cases, does not appear to be violated [14]. However, the absence of replicates prevented further confirmation by Bartlett's Test.

Normality Test

Similarly, using MINITAB a normal probability plot was generated to test the normality assumption. The results obtained for both regression models are shown in Figures 30 and 31 respectively.

a. Maximum Principal Stress Regression Model

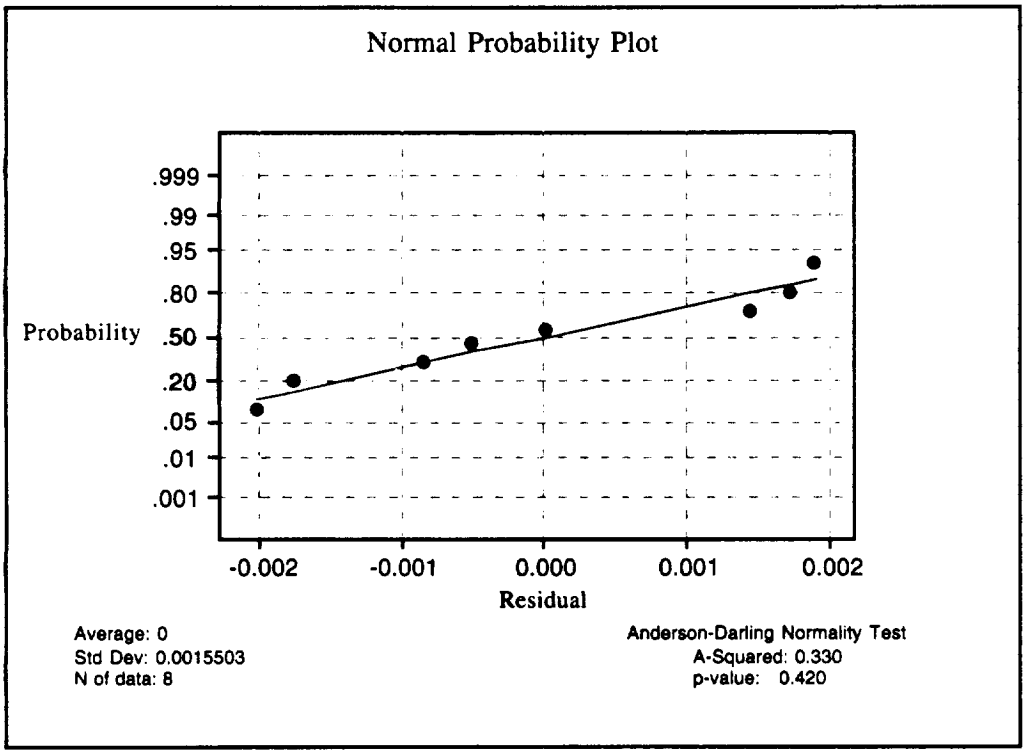

Figure 30. Normal Probability Plot: Maximum Principal Stress

b. Maximum Deflection Regression Model

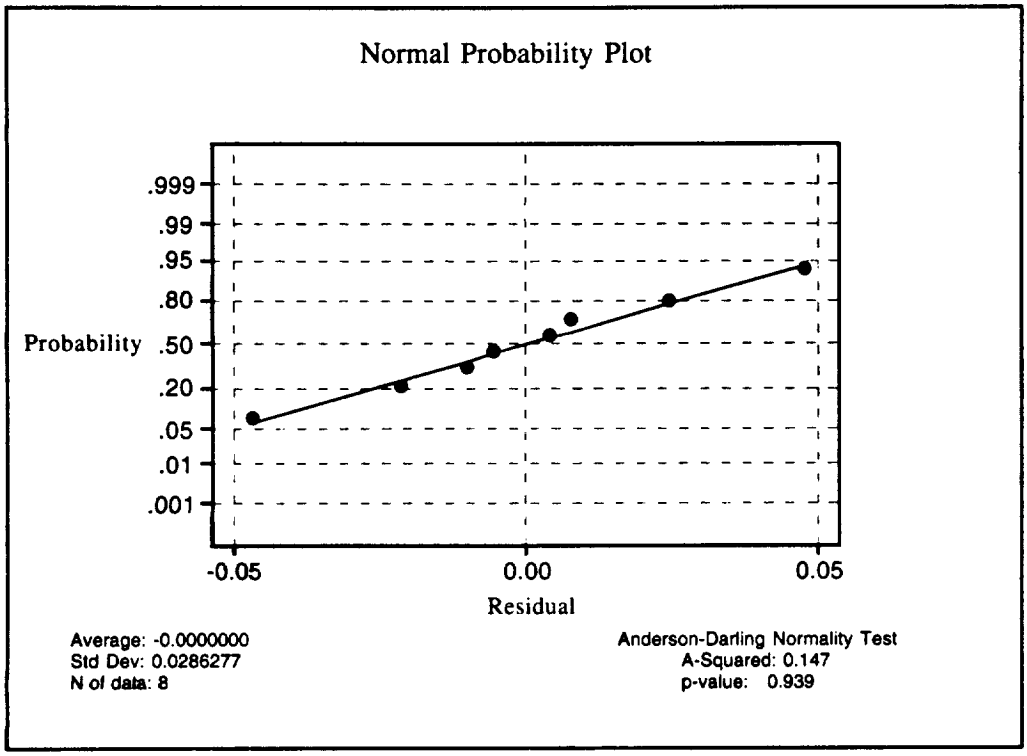

Figure 31. Normal Probability Plot: Maximum Deflection

- **Conclusion**

The normal probability plots of both Figures 30 and 31 do not suggest a serious departure from a straight-line, thereby implying that the normality assumption, in both cases, does not appear to be violated [16]. Note a p-value > 0.10 for both cases. A further indication that there is not enough evidence to reject the null hypothesis of normality.

Chapter VI. NUMERICAL OPTIMIZATION

In order to develop a reliability based multi-objective design tool, nonlinear single and multi-objective constrained optimization techniques were applied to the design of a pressure vessel cover plate. In this chapter the complete optimization process, as previewed in Chapter III, is presented. In particular, the generalized nonlinear constrained optimization problem, in reference to sequential unconstrained minimization and nonlinear goal programming, is presented along with the optimization methods adopted for solution. In each case, several numerical test cases were solved and the proceeding sections detail their development.

6.1 Sequential Unconstrained Minimization

General Nonlinear Constrained Optimization Problem Formulation

The classical optimization method has its roots in the study of maxima and minima of functions and functionals [11]. Based on this method, the general nonlinear constrained optimization problem is formulated as follows [1]:

Minimize:	$F(\mathbf{X})$		objective function	
Subject to:				
	$g_j(\mathbf{X}) \le 0$	$j = 1, m$	inequality constraints	
	$h_k(\mathbf{X}) = 0$	$k = 1, l$	equality constraints	(6-1)
	$X_i^l \le X_i \le X_i^u$	$i = 1, n$	side constraints	
To find:	$\mathbf{X} = \{X_1, X_2, X_3, ..., X_n\}$		design variables	

SUMT - Linear Extended Interior Penalty Function Method

Over the years, various methods have been proposed/developed to solve the general nonlinear constrained optimization problem of Eq. (6-1). A notable approach, given the simplicity of its optimization strategy, has been the development of the so-called sequential unconstrained minimization techniques or SUMT.

As the name implies, SUMT require the solution of several unconstrained minimization subproblems in order to obtain the optimum constrained design [1]. The basic underlying principle of SUMT is to minimize the objective function as an unconstrained function but at the same time provide a penalty to limit constraint violations [1]. Numerically this is accomplished through the unconstrained minimization of a pseudo-objective function of the form [1]

$$\Phi(\mathbf{X}, r_p) = F(\mathbf{X}) + r_p P(\mathbf{X}) \tag{6-2}$$

where $F(\mathbf{X})$ is the original objective function, $P(\mathbf{X})$ is an imposed penalty function, and r_p is a scalar multiplier that determines the magnitude of the penalty imposed for a given unconstrained minimization cycle.

The specific form that the penalty function assumes characterizes each SUMT. A notable approach in this context is the linear extended interior penalty function method. A method that when compared with other classical approaches (e.g. exterior and interior penalty methods) has proven to be far more efficient and reliable at obtaining an improved design [1].

As developed by Cassis and Schmit [1], the linear extended interior penalty function method provides for a penalty function (assuming the absence of equality constraints) of the form [1]

$$P(\mathbf{X}) = \sum_{j=1}^{m} \tilde{g}_j(\mathbf{X}) \tag{6-3a}$$

where

$$\tilde{g}_j(\mathbf{X}) = -\frac{1}{g_j(\mathbf{X})} \qquad \text{if } g_j(\mathbf{X}) \le \varepsilon \tag{6-3b}$$

$$\tilde{g}_j(\mathbf{X}) = -\frac{2\varepsilon - g_j(\mathbf{X})}{\varepsilon^2} \qquad \text{if } g_j(\mathbf{X}) > \varepsilon \tag{6-3c}$$

The parameter ε, as defined by Haftka and Starnes [1], is defined by

$$\varepsilon = -C(r_p)^a \qquad \tfrac{1}{3} \le a \le \tfrac{1}{2} \tag{6-4}$$

where C is a constant.

In Figure 32, the algorithm for the linear extended interior penalty function method is presented. Parameters of interest including $\mathbf{X}^0$, r_p, γ, C, and a are user defined, and the interested reader is referred to Vanderplaats [1] for an in depth discussion into their specific selection.

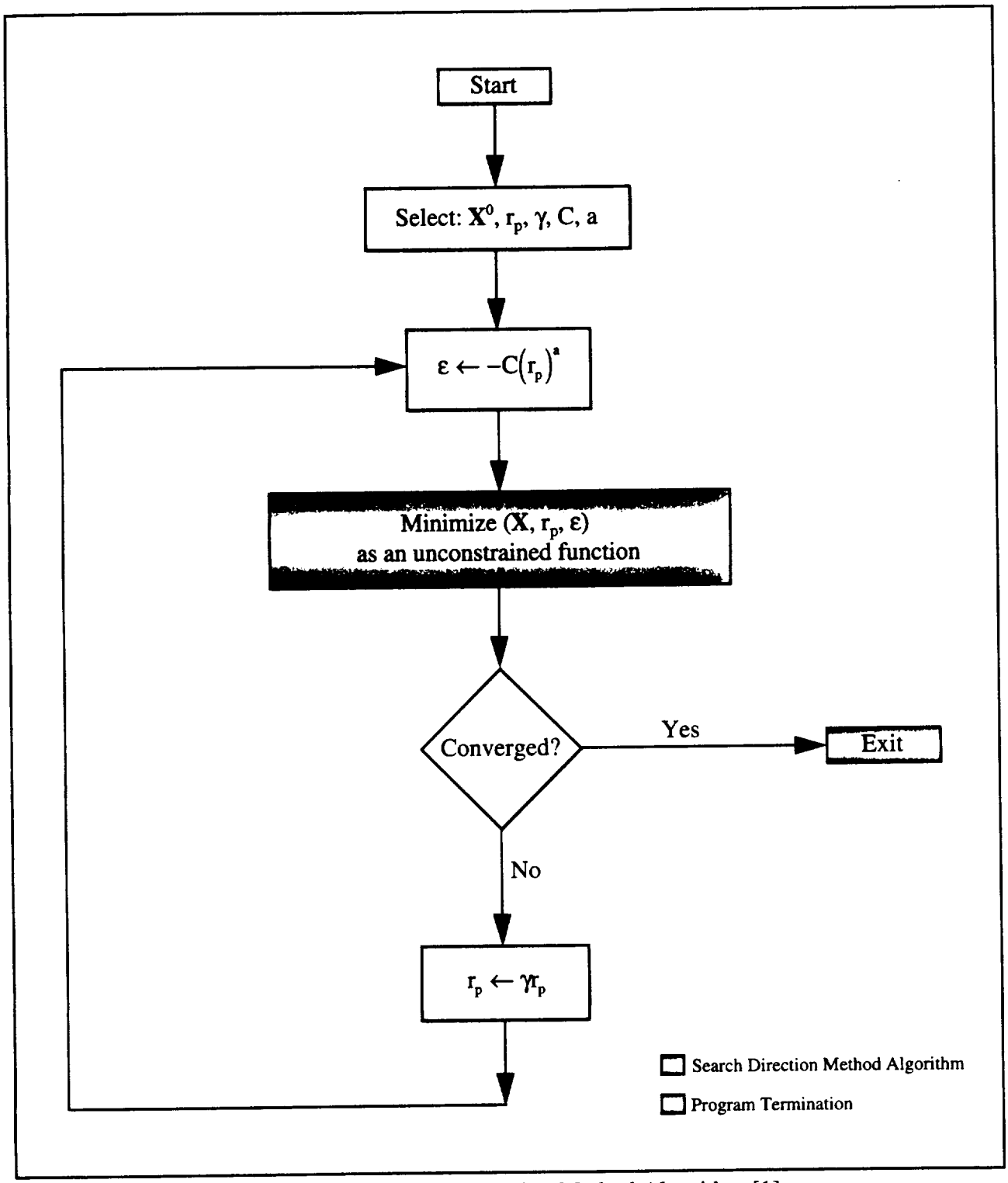

Figure 32. Linear Extended Interior Penalty Function Method Algorithm [1]

Unconstrained Minimization - First Order Methods

As noted earlier and as shown by the algorithm of Figure 32, SUMT require the solution of several unconstrained minimization subproblems, as defined by Eq. (6-2), in order to obtain the optimum constrained design as defined by Eq. (6-1). In this section, two first order unconstrained minimization methods are discussed, namely steepest descent and variable metric.

The steepest descent and variable metric methods are first order (i.e. gradient based) numerical search techniques. These techniques start from an initial design vector $\mathbf{X}^0$ and iteratively update the design until no more progress can be made to improve (minimize) the objective function. The most common form [1] of this iterative procedure is given by

$$\mathbf{X}^{q+1} = \mathbf{X}^q + \alpha_q^* \mathbf{S}^q \qquad (6\text{-}5)$$

where q is the iteration number, $\mathbf{X}$ is the vector of design variables, $\mathbf{S}^q$ is the search direction vector, and α_q^* is a scalar multiplier determining the amount of change in $\mathbf{X}$ for a given iteration.

The specific form of the search direction vector (i.e. search engine) determines the type of search method employed. In the case of the steepest descent method, the search direction is taken as the negative of the gradient of the objective function [1]. That is, at iteration q

$$\mathbf{S}^q = -\nabla F(\mathbf{X}^q) \qquad (6\text{-}6)$$

Variable metric methods [1], on the other hand, define the search direction at iteration q by

$$\mathbf{S}^q = -\mathbf{H}\,\nabla F(\mathbf{X}^q) \qquad (6\text{-}7)$$

where $\mathbf{H}$ is an n dimensional array whose form defines the specific variable metric method employed. Vanderplaats [1] presents a complete discussion on this topic and is listed here for further reference. However, it should be noted that the $\mathbf{H}$ matrix plays a pivotal role in accelerating the rate of convergence, as compared to the steepest descent method, by utilizing information from previous iterations. As a result, variable metric methods, such as the Broydon-Fletcher-Goldfarb-Shanno (BFGS) method, are recommended for general applications in favor of the steepest descent method [1].

In Figure 33, the algorithm for the steepest descent and variable metric methods is shown. Regardless of the search engine employed, the algorithm consists of three major components [1]

1. Determine the direction in which to search (i.e. select search engine)
2. Perform the resulting one-dimensional search
3. Check for convergence (i.e. attainment of an acceptable solution)

One-Dimensional Search - Golden Section Method

Based on Eq. (6-5) in conjunction with the algorithm of Figure 33, the unconstrained minimization problem in n variables eventually reduces to a one-dimensional search in α^*. In this section, a brief summary of a one-dimensional search technique based on the golden section method is presented.

The basic strategy behind a one-dimensional unconstrained minimum search method can best be summarized by the general flowchart shown in Figure 34. The three major components of interest include

1. **The Bounding Algorithm**: ensures that in the region of search the function is unimodal. That is, the function has only one bounded minimum solution.
2. **The Golden Section Method Algorithm**: reduces/refines the bounded interval to an optimum minimum size. Three optimum points define this optimum minimum interval.
3. **Polynomial Interpolation**: refines solution through a three-point quadratic approximation. Yields α^*.

In Figures 35 and 36, the flowcharts for both the bounding algorithm and the golden section method are shown respectively. There are presented here only for reference since a detailed explanation is beyond the scope of this paper.

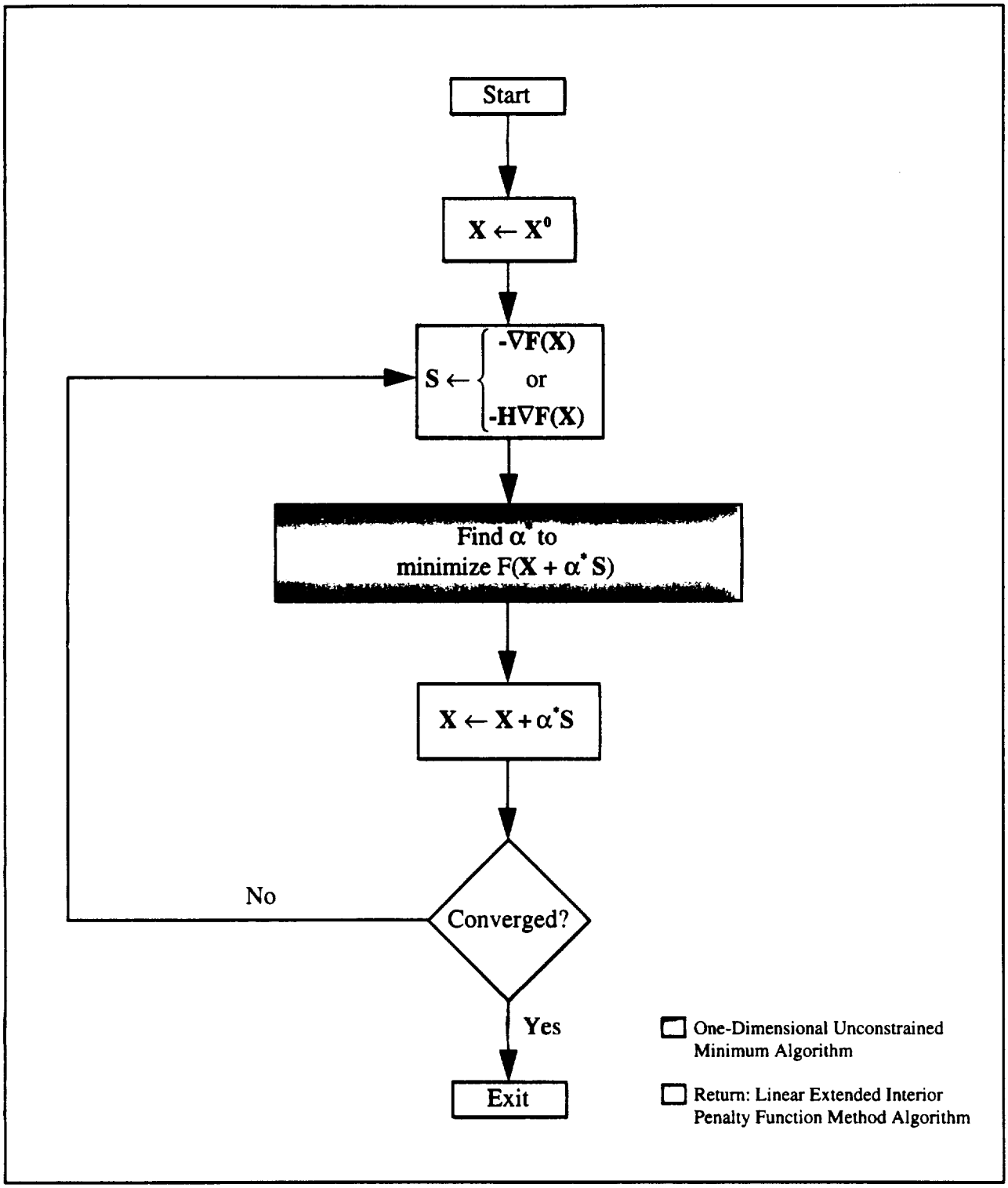

Figure 33. Search Direction Method Algorithm [1]

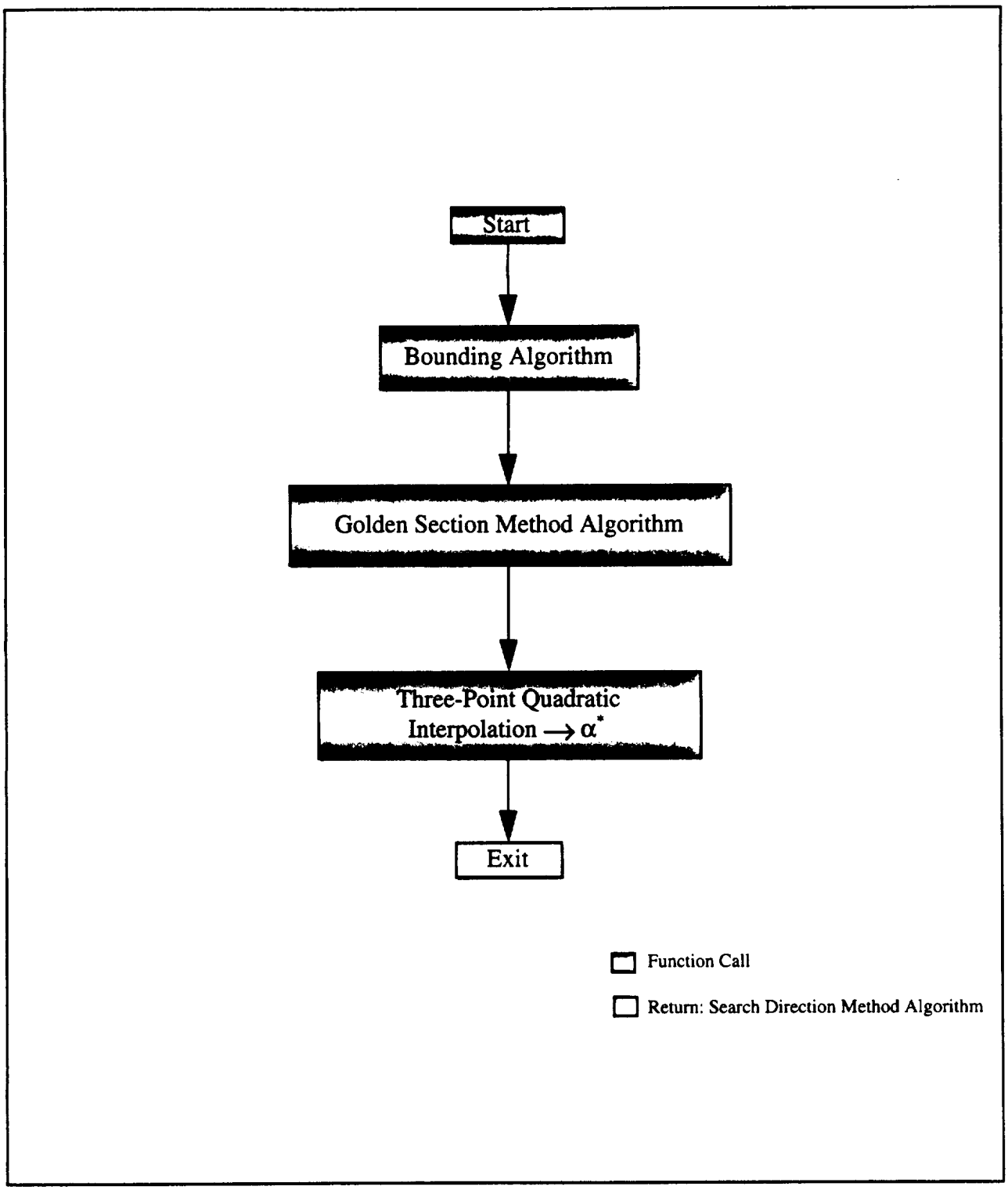

Figure 34. One-Dimensional Unconstrained Minimum Algorithm [1]

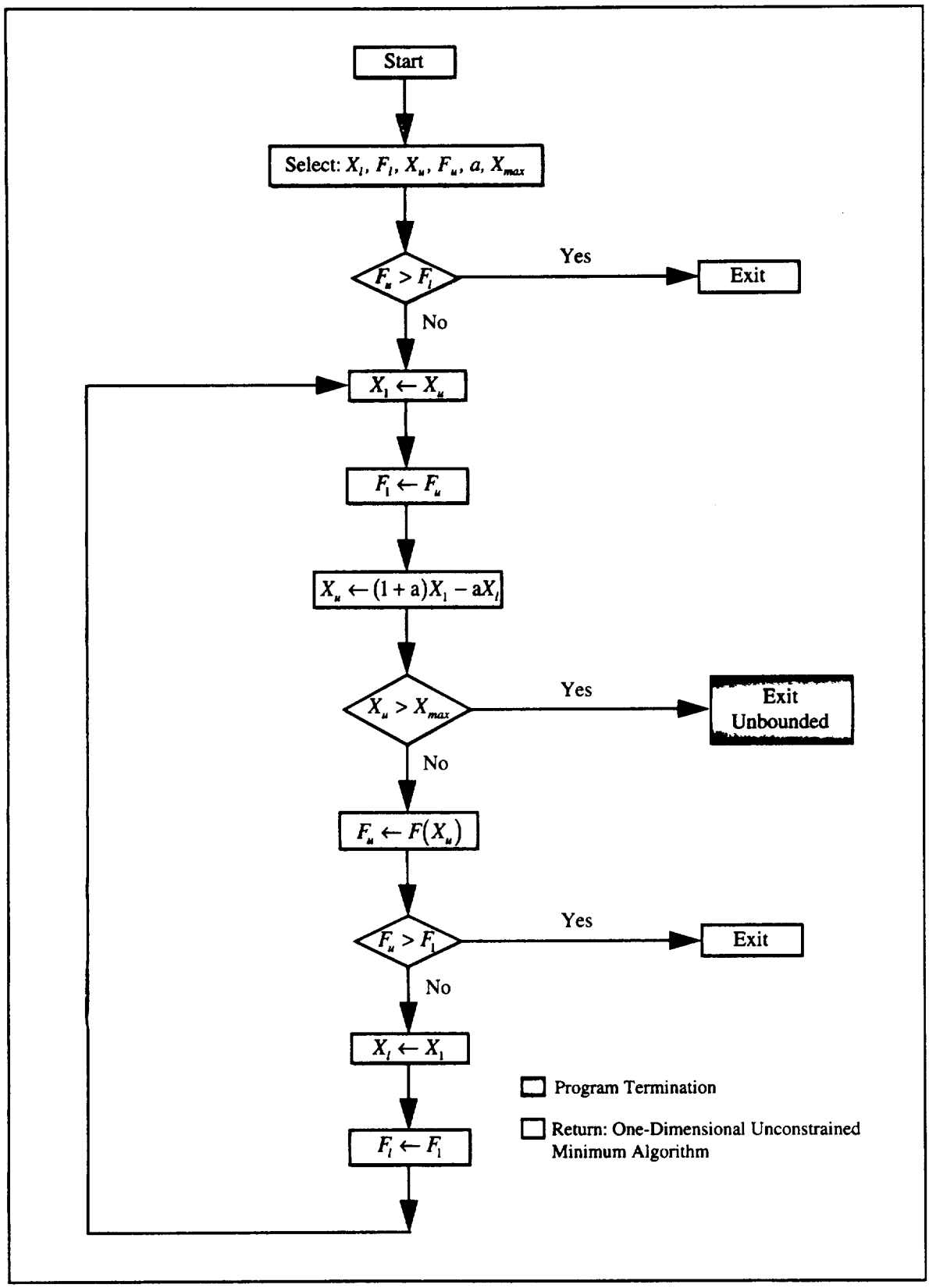

Figure 35. Unconstrained Minimum Bounding Algorithm [1]

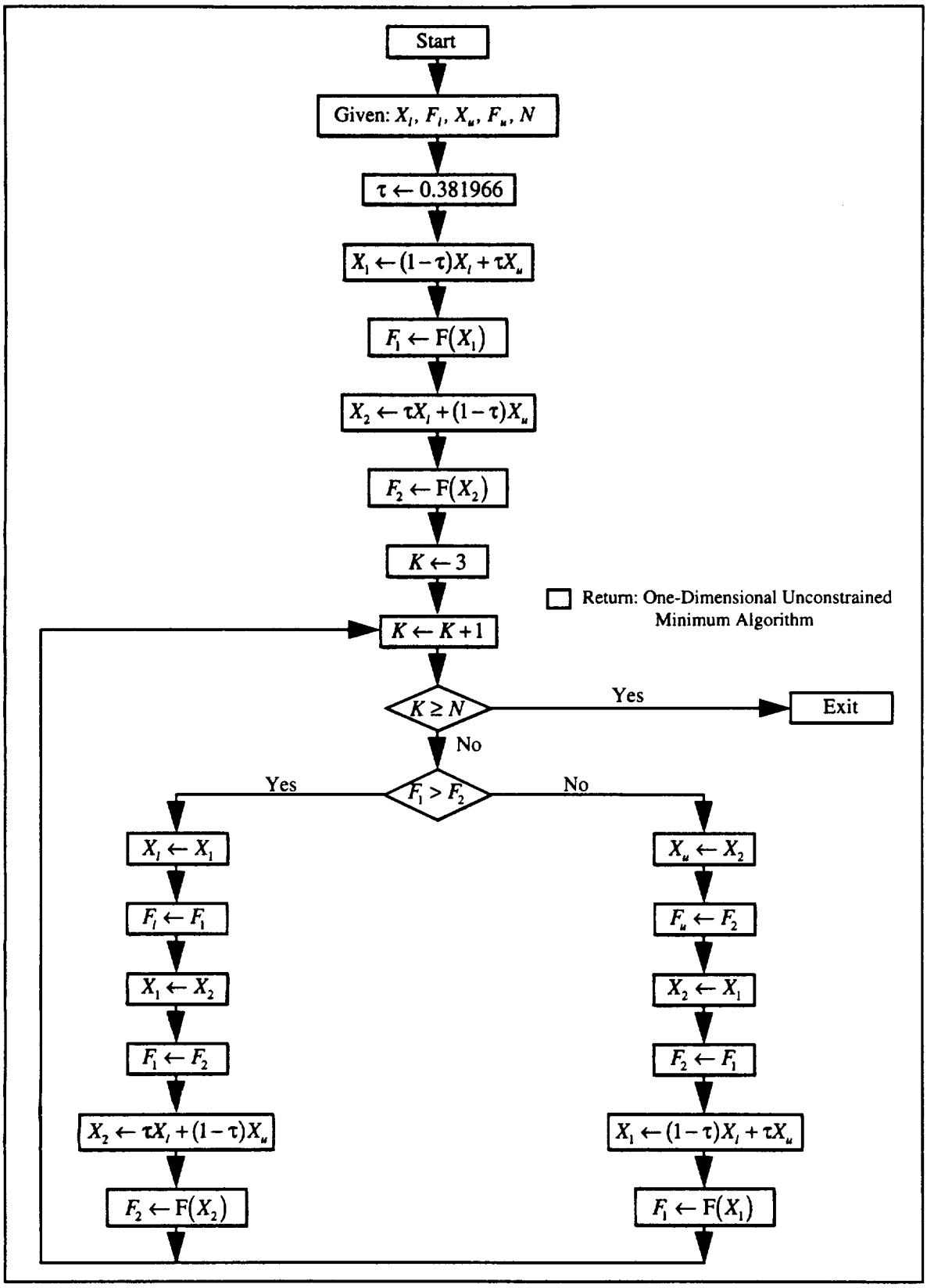

Figure 36. Golden Section Algorithm [1]

Convergence Criteria

Convergence criteria play a pivotal role in the optimization routines of Figures 32 and 33 given that they determine program termination. Specifically, they assess whether convergence to an acceptable solution has been achieved, and as a consequence have a major effect on the efficiency and reliability of these optimization techniques [1]. In this section a convergence algorithm is presented and its associated convergence criteria are briefly discussed.

In Figure 37, an algorithm for assessing convergence is presented. It incorporates three convergence (termination) criteria [1], namely

1. **Maximum Number of Iterations**: $q \geq q_{max}$

   This termination criterion is provided in order to ensure that the optimization algorithm will not continue to iterate indefinitely. In essence, it is simply a safety feature ensuring program termination.

2. **Absolute Change in the Objective Function**: $|F(\mathbf{X}^q) - F(\mathbf{X}^{q-1})| \leq \varepsilon_A$

   This termination criterion checks on the progress of the optimization. Specifically, it compares the absolute value of the objective function $F(\mathbf{X})$ on successive iterations. Convergence is achieved if the absolute change is within a specified tolerance, $\varepsilon_A \approx 0.0001$ (user defined parameter).

3. **Relative Change in the Objective Function**: $\dfrac{|F(\mathbf{X}^q) - F(\mathbf{X}^{q-1})|}{\max[|F(\mathbf{X}^q)|, 10^{-10}]} \leq \varepsilon_R$

   Similar to the absolute change criterion, this termination criterion checks on the progress of the optimization. However, this criterion compares the relative change in the objective function $F(\mathbf{X})$ between successive iterations. Convergence is achieved if the relative change is within a specified tolerance, $\varepsilon_R \approx 0.001$ (user defined parameter).

Lastly, it should be noted that convergence is indicated when either the absolute or relative change criterion are satisfied. However, in order to ensure true convergence it is important that the criterion be satisfied on at least two successive iterations [1].

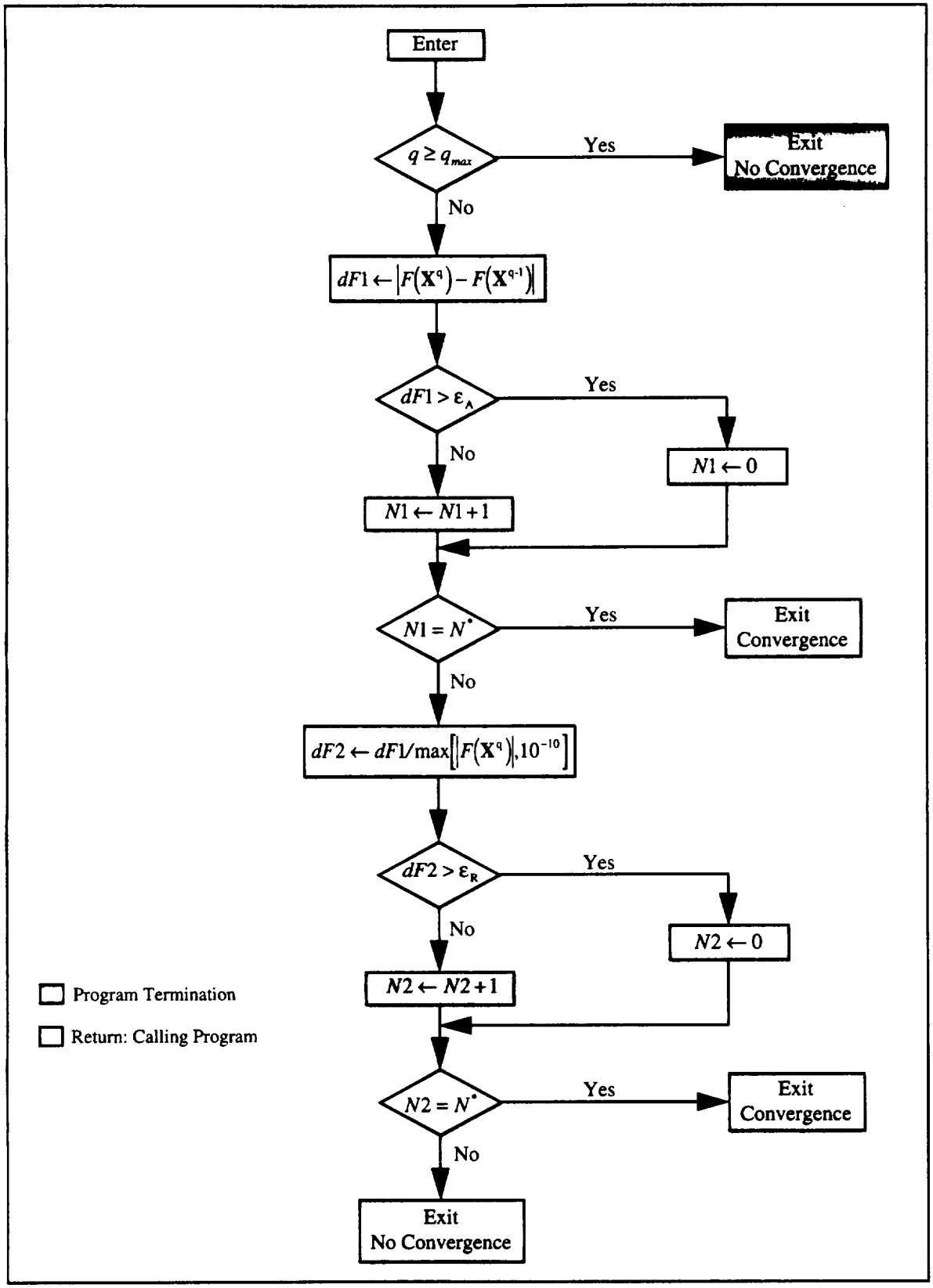

Figure 37. Convergence Algorithm [1]

6.2 SUMT - Reliability Based Optimization

A reliability based nonlinear constrained optimization design tool was developed based on the linear extended interior penalty function method (SUMT). The BFGS variable metric method was used for the unconstrained minimization subproblem, and the one-dimensional search used the golden section method followed by three-point quadratic polynomial interpolation. Convergence criteria included maximum number of iterations and absolute and relative change criterion. Both single and multi-objective numerical test cases were conducted as applied to the design of a pressure vessel cover plate. In the following sections the results obtained are presented.

SUMT - Nonlinear Single Objective Constrained Optimization

A nonlinear single objective constrained optimization design problem was undertaken in order to address two main objectives: (1) ensure predicted optimum design was within ASME Code standards and (2) assess how the variability in the strength characteristics of the cover plate affected the predicted optimum. In particular, based upon the preselected design criteria (see: Chp. II) in conjunction with the required service conditions (see: Chp. III), the single objective design problem focused on minimizing the structural weight of the cover plate, as a function of its thickness, subject to constraints on stress, deflection, and reliability. That is, find the design variable, h, that would

$$\begin{aligned} &\text{Minimize:} && W(h) = \rho A h \\ &\text{Subject to:} \\ & && g_1(h) = \frac{\sigma}{\sigma_{max}} - 1 \le 0 \\ & && g_2(h) = \frac{z}{z_{max}} - 1 \le 0 \\ & && g_3(h) = 1 - \frac{R}{R_o} \le 0 \end{aligned} \qquad (6\text{-}8)$$

where
- $\rho = 7.86 \times 10^{-6}$ kg/mm^3
- $A = \frac{\pi D^2}{4}$
- $\sigma = \sigma(h) = 28716h^{-2.0}$ [see: Eq. (5-7)]
- $\sigma_{max} = 120$ MPa
- $z = z(h) = 331.68h^{-3.0}$ [see: Eq. (5-9)]
- $z_{max} = 0.1$ mm
- $R = R(h) = R(\sigma, S)$ [see: Figure 5]
- $R_o = 0.999$

The statistical strength and stress distribution parameters were assumed as follows

- $S \sim N(\mu_s, \hat{\sigma}_s)$: strength at the critical location in the plate
  - $\mu_s \approx S_y = 262$ MPa
  - $\hat{\sigma}_s = 5$ MPa
- $\sigma \sim N(\mu_\sigma, \hat{\sigma}_\sigma)$: load induced stress at the critical location in the plate
  - $\mu_\sigma \approx \sigma(h) = 28716h^{-2.0}$
  - $\hat{\sigma}_\sigma = 2$ MPa

Penalty parameters included: $r_p = 1.5$, $\varepsilon_i = -0.1$, $a = 0.5$, and $\gamma = 0.1$.

Test Cases

Case I. ASME Code Verification

The nonlinear single objective constrained optimization problem of Eq. (6-8) was solved using the developed SUMT design tool in order to verify that the predicted optimum design was within ASME Code standards. In particular, the predicted optimum design was compared with the specifications provided for by Eq. (1-1) per ASME Code UG-34 and UW-12 [9]. In Table 4, the results of this comparison are presented.

Table 4. ASME Code Verification Data

Design	Maximum Allowable Joint Efficiency, E	Minimum Allowable Thickness, h(mm)	Structural Weight W(h), kg
ASME: Fully Radiographed	0.90[a]	14.18[c]	3.50
ASME: Spot Examined	0.80[a]	15.04[c]	3.71
SUMT: Optimum	0.76[b]	15.47	3.82
ASME: Not Examined	0.65[a]	16.69[c]	4.12

[a] Per ASME Code UW-12 [9]; [b] Theoretical: Computed based on Eq.(1-1); [c] Per ASME Code UG-34 [9]: Eq.(1-1)

- **Conclusion**

The SUMT design optimum was within ASME specifications. Primarily: (1) the SUMT optimum did not require a maximum allowable joint efficiency greater than that provided for by the ASME Code (i.e. E = 0.9), and (2) the SUMT minimum optimum thickness did not violate the minimum allowable thickness per ASME Code (i.e. h =14.18 mm). It should be noted that the importance of the results listed in Table 4 lie not on whether the SUMT design was better

than or worse than the ASME designs, but rather on the observation that the SUMT design was in compliance with ASME specifications, namely maximum allowable joint efficiency and minimum allowable plate thickness. Simply stated, the SUMT design tool provided for a design that satisfied the required user specified design criteria (e.g. load induced stress and deflection and reliability), while at the same time provided for a design within ASME Code specifications.

Case II. Variability Effects

Similarly, the nonlinear single objective constrained optimization problem of Eq. (6-8) was solved using the developed SUMT design tool in order to verify its ability to take into account the effects of variability on the predicted optimum. For simulation purposes the mean strength of the cover plate was varied, and as a consequence its affect on the optimum minimum thickness was recorded as listed in Table 5.

Table 5. Variability Effects Data

Test Case	Mean Strength μ_s, MPa	Minimum Allowable Thickness, h(mm)	Structural Weight W(h), kg
1	$S_y = 262^a$	15.47	3.82
2	$\frac{1}{2} S_y = 131$	15.85	3.91
3	$\frac{1}{3} S_y = 87.3$	20.39	5.03
4	$\frac{1}{4} S_y = 65.5$	24.42	6.03

[a] SA-515-70 grade carbon steel [9]

• Conclusion

The developed SUMT design tool provided for an optimum design suited to the specified strength statistic, μ_s. By varying this statistical parameter, its affect on the predicted optimum was accounted for.

SUMT - Nonlinear Multi-Objective Constrained Optimization

A nonlinear multi-objective constrained optimization design problem was undertaken in order to assess how the selection of weighting factors, in reference to conflicting and multiple objectives, affected the predicted optimum design. In particular, the multi-objective design problem focused on minimizing the structural weight, load induced stress and deflection, and maximizing the reliability of the preselected cover plate, as a function of its thickness, subject to constraints on stress, deflection, and reliability. That is, find the design variable, h, that would

$$\text{Minimize:} \quad F(h) = \left\{ w_1 \frac{W(h)}{W_i(h)} + w_2 \frac{\sigma(h)}{\sigma_i(h)} + w_3 \frac{z(h)}{z_i(h)} - w_4 \frac{R(h)}{R_i(h)} \right\}$$

Subject to:

$$g_1(h) = \frac{\sigma}{\sigma_{max}} - 1 \leq 0$$

$$g_2(h) = \frac{z}{z_{max}} - 1 \leq 0 \qquad (6\text{-}9)$$

$$g_3(h) = 1 - \frac{R}{R_o} \leq 0$$

where

- w_n (for n = 1, 2, 3, 4): weighting factors
- $W(h) = \rho A h$
- $\rho = 7.86 \times 10^{-6}$ kg/mm^3
- $A = \frac{\pi D^2}{4}$
- $\sigma = \sigma(h) = 28716 h^{-2.0}$ [see: Eq. (5-7)]
- $\sigma_{max} = 120$ MPa
- $z = z(h) = 331.68 h^{-3.0}$ [see: Eq. (5-9)]
- $z_{max} = 0.1$ mm
- $R = R(h) = R(\sigma, S)$ [see: Figure 5]
- $R_o = 0.999$
- ith subscript indicates function value at initial value of design variable

The statistical strength and stress distribution parameters were assumed as follows

- $S \sim N(\mu_s, \sigma_s)$: strength at the critical location in the plate
  - $\mu_s \approx S_y = 262$ MPa
  - $\sigma_s = 5$ MPa

• $\sigma \sim N(\mu_\sigma, \hat{\sigma}_\sigma)$: load induced stress at the critical location in the plate

• $\mu_\sigma \approx \sigma(h) = 28716h^{-2.0}$ • $\hat{\sigma}_\sigma = 2$ MPa

Penalty parameters included: $r_p = 1.5$, $\varepsilon_i = -0.1$, $a = 0.5$, and $\gamma = 0.1$.

Test Cases

The nonlinear multi-objective constrained optimization problem of Eq. (6-9) was solved using the developed SUMT design tool in order to verify its ability to take into account conflicting and multiple objectives. For simulation purposes the specified weighting factors were varied, and as a consequence their affect on the predicted optimum minimum thickness was recorded as listed in Table 6.

Table 6. Impact of Weighting Factors on Optimum Design

Test Case	w_1	w_2	w_3	w_4	Minimum Allowable Thickness, h(mm)	Structural Weight W(h), kg	Stress σ(h), MPa	Deflection z(h), mm	Reliability R(h)
1	5.0	0.0	0.0	0.0	15.47	3.82	na	na	na
2	2.0	5.0	1.0	1.0	27.01	6.67	39.36	0.017	0.9999
3	5.0	2.0	1.0	0.0	16.55	4.09	104.79	0.073	na
4	5.0	1.0	2.0	5.0	17.01	4.20	99.24	0.067	0.9999

na: not applicable

• Conclusion

The developed SUMT design tool provided for an optimum design suited to the specified weight ordered design objectives. Multiple and conflicting objectives, namely structural weight, load induced stress and deflection, and reliability were accounted for.

6.3 Nonlinear Goal Programming

General Nonlinear Goal Programming Problem Formulation

The standard form of the nonlinear constrained optimization goal programming model is formulated as follows [2]:

$$\text{Minimize: } \mathbf{z} = \begin{Bmatrix} f_1(d^-, d^+) \\ f_2(d^-, d^+) \\ \cdot \\ \cdot \\ f_K(d^-, d^+) \end{Bmatrix} \qquad \text{achievement vector}$$

Subject to:

$$\begin{aligned} & g_i(\mathbf{X}) + d_i^- - d_i^+ = b_i && i = 1, I && \text{design constraints} \\ & d_i^-, d_i^+ \geq 0 && i = 1, I && \text{nonnegativity requirement} \\ & X_i^l \leq X_i \leq X_i^u && i = 1, n && \text{side constraints} \end{aligned} \qquad (6\text{-}10)$$

To find: $\mathbf{X} = \{X_1, X_2, X_3, ..., X_n\}$ design variables

The simplified nonlinear constrained optimization goal programming model is written as [2]:

$$\text{Minimize: } \mathbf{z} = \begin{Bmatrix} \text{weighted deviations of Priority 1} = P_1 \\ \text{weighted deviations of Priority 2} = P_2 \\ \cdot \\ \cdot \\ \text{weighted deviations of Priority K} = P_K \end{Bmatrix}$$

Subject to:

$$\begin{aligned} & \text{Design Criteria 1} - \text{Target for Criteria 1} = \text{deviation 1} \\ & \text{Design Criteria 2} - \text{Target for Criteria 2} = \text{deviation 2} \\ & \vdots \\ & \text{Design Criteria I} - \text{Target for Criteria I} = \text{deviation I} \end{aligned} \qquad (6\text{-}11)$$

In addition to,

Nonegativity requirement on deviations,

Side constraints

To find: $\mathbf{X} = \{X_1, X_2, X_3, ..., X_n\}$

The vector **z** is referred to as the achievement vector. It is structured as an ordered set such that a preemptive priority structure is maintained [2]. That is, P_1 (most important goal) > P_2 >>> P_K (least important goal) [17]. The dimension of **z** represents the number of preemptive priority levels which is equal to or less than the number of objectives (design criteria), and the value of **z** will be equal to the zero vector if all the objectives meet their targets [2]. Lastly, it is important to note for clarity that in reference to Eq. (6-10), $g_i(\mathbf{X})$ represent the design objectives (criteria) and b_i the aspired targets.

NLGP - Powell's Conjugate Directions Method

As noted earlier, a variety of methods have been proposed/developed over the years to solve nonlinear optimization problems. One such approach, namely the linear extended interior penalty function method, was introduced in Sect. 6.1. In this section, an alternative approach for solving the nonlinear goal programming problem of Eq. (6-11) is introduced, namely Powell's conjugate directions method. A method that is one of the most efficient and reliable and certainly the most popular of the zero-order (i.e. nongradient) based methods available today [1, 2].

Based on the concept of conjugate directions, Powell's method is a zero-order unconstrained minimization numerical search technique [1]. As was the case with the first-order methods introduced earlier, this technique starts from an initial design vector $\mathbf{X}^0$ and iteratively updates the design until no more progress can be made to improve (minimize) the objective function or in the case of Eq. (6-11) the achievement vector.

Following the updating formula of Eq. (6-5), the basic concept of Powell's method is first to search in n orthogonal directions, where each search consists of updating the design vector using the minimum along the previous search direction as the starting point [2]. After performing these successive minimizations, a new search direction is formed between the original starting point and the resulting point of the successive n searches. The first search direction is then dropped and the remaining search directions are kept along with the new direction, which is placed last among the directions. The search is continued until convergence is achieved.

6.4 NLGP - Reliability Based Optimization

A reliability based nonlinear optimization design tool for solving the nonlinear goal programming (NLGP) problem of Eq. (6-11) was developed based on Powell's conjugate directions method. The developed NLGP design tool first minimizes, as nearly as possible, the objectives with the highest priority level. It then proceeds to satisfy the objectives of the next priority, as nearly as possible, without degrading the achievement of any objective in a higher priority level. This process is continued until all priority levels have been considered.

At each priority level the search is terminated when the difference between the present and the previous achievement function value becomes sufficiently small. The value of the achievement vector **z** will be equal to the zero vector if all the objectives meet their preselected targets.

Test Cases

In an effort to demonstrate the capabilities of the developed NLGP design tool several numerical test cases, as applied to the design of a pressure vessel cover plate, were conducted. In particular, based upon the preselected design criteria (see: Chp. II) in conjunction with the required service conditions (see: Chp. III), four test cases were run including: (i) minimum weight design with reliability constraints only; (ii) minimum weight design with stress and reliability constraints at different priority levels; (iii) minimum weight design with deflection and reliability constraints at different priority levels; and (iv) minimum weight design with stress, deflection, and reliability constraints at different priority levels. In all four cases the maximum positive or negative deviation was limited to be less than 0.01. In the following sections the results obtained are presented.

Case I. Minimum Weight Design with Reliability Constraints

The minimum weight design problem with reliability constraints was solved using the developed NLGP design tool. In particular, the optimization problem focused on minimizing the structural

weight of the preselected cover plate as a function of its thickness subject to reliability constraints. That is, find the design variable, h, that would

Minimize: $\mathbf{z} = \{\text{deviation 1} + \text{deviation 2}\}$ Achievement Vector

Subject to:

$$\frac{W}{W_o} - 1 = \text{deviation 1}$$

$$\frac{R}{R_o} - 1 = \text{deviation 2}$$

Design Constraints

and side constraints

$$5 \leq h \leq 40$$

where

- $W \geq W_o$
- $W = W(h) = \rho A h$
- $A = \frac{\pi D^2}{4}$
- $R = R(h) = R(\sigma, S)$ [see: Figure 5]
- $R \geq R_o$
- $\rho = 7.86 \times 10^{-6}$ kg/mm^3
- $W_o = 3.50$ kg
- $R_o = 0.999$

The statistical strength and stress distribution parameters were assumed as follows

- $S \sim N(\mu_s, \hat{\sigma}_s)$: strength at the critical location in the plate
  - $\mu_s \approx S_y = 262$ MPa
  - $\hat{\sigma}_s = 5$ MPa
- $\sigma \sim N(\mu_\sigma, \hat{\sigma}_\sigma)$: load induced stress at the critical location in the plate
  - $\mu_\sigma \approx \sigma(h) = 28716h^{-2.0}$
  - $\hat{\sigma}_\sigma = 2$ MPa

In Table 7, the predicted optimum minimum thickness along with the optimum weight and the expected reliability for the cover plate design are listed.

Table 7. Results for Case I - NLGP Cover Plate Design

Minimum Optimum Thickness, h(mm)	Structural Weight W(h), kg	Reliability R(h)
14.20	3.51	0.9999

Case II. Minimum Weight Design with Stress and Reliability Constraints

In this case, the minimum weight design problem with reliability and stress constraints at different priority levels was solved using the developed NLGP design tool. Specifically, the optimization problem focused on minimizing the structural weight of the preselected cover plate as a function of its thickness with: (i) weight and stress constraints priority level 1; and (ii) reliability constraints priority level 2. That is, find the design variable, h, that would

Minimize: $\mathbf{z} = \begin{Bmatrix} \text{deviation 1} + \text{deviation 2} \\ \text{deviation 3} \end{Bmatrix}$ Achievement Vector

Subject to:

$$\frac{W}{W_o} - 1 = \text{deviation 1}$$

$$\frac{\sigma}{\sigma_{max}} - 1 = \text{deviation 2} \qquad \text{Design Constraints}$$

$$\frac{R}{R_o} - 1 = \text{deviation 3}$$

and side constraints

$$5 \leq h \leq 40$$

where

- $W \geq W_o$
- $R \geq R_o$
- $A = \frac{\pi D^2}{4}$
- $\sigma = \sigma(h) = 28716h^{-2.0}$ [see: Eq. (5-7)]
- $R = R(h) = R(\sigma, S)$ [see: Figure 5]
- $\sigma \leq \sigma_{max}$
- $W = W(h) = \rho Ah$
- $W_o = 3.50$ kg
- $\sigma_{max} = 120$ MPa
- $R_o = 0.999$

The statistical strength and stress distribution parameters were assumed as follows

- $S \sim N(\mu_s, \hat{\sigma}_s)$: strength at the critical location in the plate
  - $\mu_s \approx S_y = 262$ MPa
  - $\hat{\sigma}_s = 5$ MPa
- $\sigma \sim N(\mu_\sigma, \hat{\sigma}_\sigma)$: load induced stress at the critical location in the plate
  - $\mu_\sigma \approx \sigma(h) = 28716h^{-2.0}$
  - $\hat{\sigma}_\sigma = 2$ MPa

In Table 8, the predicted optimum minimum thickness along with the optimum weight and the expected maximum principal stress and reliability for the cover plate design are listed.

Table 8. Results for Case II - NLGP Cover Plate Design

Minimum Optimum Thickness, h(mm)	Structural Weight W(h), kg	Maximum Principal Stress σ(h), MPa	Reliability R(h)
15.47	3.82	120.0	0.9999

Case III. Minimum Weight Design with Deflection and Reliability Constraints

In this case, the minimum weight design problem with deflection and reliability constraints at different priority levels was solved using the developed NLGP design tool. In particular, the optimization problem focused on minimizing the structural weight of the preselected cover plate as a function of its thickness with: (i) weight and deflection constraints priority level 1; and (ii) reliability constraints priority level 2. That is, find the design variable, h, that would

Minimize: $\mathbf{z} = \begin{Bmatrix} \text{deviation 1} + \text{deviation 2} \\ \text{deviation 3} \end{Bmatrix}$ Achievement Vector

Subject to:

$$\frac{W}{W_o} - 1 = \text{deviation 1}$$

$$\frac{z}{z_{max}} - 1 = \text{deviation 2} \qquad \text{Design Constraints}$$

$$\frac{R}{R_o} - 1 = \text{deviation 3}$$

and side constraints

$$5 \leq h \leq 40$$

where

- $W \geq W_o$
- $R \geq R_o$
- $A = \frac{\pi D^2}{4}$
- $z = z(h) = 331.68h^{-3.0}$ [see: Eq. (5-9)]
- $R = R(h) = R(\sigma, S)$ [see: Figure 5]
- $z \leq z_{max}$
- $W = W(h) = \rho Ah$
- $W_o = 3.50$ kg
- $z_{max} = 0.1$ mm
- $R_o = 0.999$

The statistical strength and stress distribution parameters were assumed as follows

- $S \sim N(\mu_s, \delta_s)$: strength at the critical location in the plate
  - $\mu_s \approx S_y = 262$ MPa
  - $\delta_s = 5$ MPa
- $\sigma \sim N(\mu_\sigma, \delta_\sigma)$: load induced stress at the critical location in the plate
  - $\mu_\sigma \approx \sigma(h) = 28716h^{-2.0}$
  - $\delta_\sigma = 2$ MPa

In Table 9, the predicted optimum minimum thickness along with the optimum weight and the expected maximum deflection and reliability for the cover plate design are listed.

Table 9. Results for Case III - NLGP Cover Plate Design

Minimum Optimum Thickness, h(mm)	Structural Weight W(h), kg	Maximum Deflection z(h), mm	Reliability R(h)
14.92	3.68	0.10	0.9999

Case IV. Minimum Weight Design with Stress, Deflection and Reliability Constraints

Lastly, the minimum weight design problem with stress, deflection, and reliability constraints at different priority levels was solved using the developed NLGP design tool. Specifically, the optimization problem focused on minimizing the structural weight of the preselected cover plate as a function of its thickness with: (i) weight and reliability constraints priority level 1; and (ii) stress and deflection constraints priority level 2. That is, find the design variable, h, that would

Minimize: $\mathbf{z} = \begin{Bmatrix} \text{deviation 1} + \text{deviation 4} \\ \text{deviation 2} + \text{deviation 3} \end{Bmatrix}$ Achievement Vector

Subject to:

$$\frac{W}{W_o} - 1 = \text{deviation 1}$$

$$\frac{\sigma}{\sigma_{max}} - 1 = \text{deviation 2}$$

$$\frac{z}{z_{max}} - 1 = \text{deviation 3}$$

$$\frac{R}{R_o} - 1 = \text{deviation 4}$$

Design Constraints

and side constraints

$$5 \leq h \leq 40$$

where

- $W \geq W_o$
- $z \leq z_{max}$
- $W = W(h) = \rho A h$
- $A = \frac{\pi D^2}{4}$
- $\sigma = \sigma(h) = 28716h^{-2.0}$ [see: Eq. (5-7)]
- $z = z(h) = 331.68h^{-3.0}$ [see: Eq. (5-9)]
- $R = R(h) = R(\sigma, S)$ [see: Figure 5]
- $\sigma \leq \sigma_{max}$
- $R \geq R_o$
- $\rho = 7.86 \times 10^{-6}$ kg/mm^3
- $W_o = 3.50$ kg
- $\sigma_{max} = 120$ MPa
- $z_{max} = 0.1$ mm
- $R_o = 0.999$

The statistical strength and stress distribution parameters were assumed as follows

- $S \sim N(\mu_s, \hat{\sigma}_s)$: strength at the critical location in the plate
  - $\mu_s \approx S_y = 262$ MPa
  - $\hat{\sigma}_s = 5$ MPa
- $\sigma \sim N(\mu_\sigma, \hat{\sigma}_\sigma)$: load induced stress at the critical location in the plate
  - $\mu_\sigma \approx \sigma(h) = 28716h^{-2.0}$
  - $\hat{\sigma}_\sigma = 2$ MPa

In Table 10, the predicted optimum minimum thickness along with the optimum weight and the expected maximum principal stress, maximum deflection and reliability for the cover plate design are listed.

Table 10. Results for Case IV - NLGP Cover Plate Design

Minimum Optimum Thickness, h(mm)	Structural Weight W(h), kg	Maximum Principal Stress σ(h), MPa	Maximum Deflection z(h), mm	Reliability R(h)
15.47	3.82	120.0	0.09	0.9999

CHAPTER VII. CONCLUSION

Based on two different optimization techniques, namely sequential unconstrained minimization (SUMT) and nonlinear goal programming (NLGP), a reliability based nonlinear optimization method for solving structural optimization problems was developed. A method that affords the design engineer the ability to take into account the effects of variability on the proposed design, while at the same time provides for a realistic design model that takes into account conflicting and multiple objectives. Multiple objectives of interest that include structural weight, load induced stress and deflection, and mechanical reliability.

As a testbed, both single and multi-objective numerical test cases were run, using the developed SUMT design method, as applied to the design of a pressure vessel cover plate. In particular, the single objective design problem focused on a minimum weight design subject to constraints on stress, deflection, and reliability. The nonlinear multi-objective design problem, on the other hand, focused on minimizing the structural weight, load induced stress and deflection, and maximizing the reliability of the preselected cover plate subject once again to constraints on stress, reliability, and deflection. The subsequent solution of these numerical test cases demonstrated the ability of the developed design tool to: (i) take into account the effects of variability on the proposed design; (ii) yield an optimum design within ASME specifications; and (iii) yield an optimum design suited to a user specified weight ordered priority system.

Similarly, in an effort to demonstrate the capabilities of the developed NLGP design tool several numerical test cases, as applied to the design of a pressure vessel cover plate, were likewise solved. These test cases ranged from a minimum weight design with reliability constraints to a minimum weight design with stress, reliability, and deflection constraints at different priority levels. As was the case with the developed SUMT method, the developed NLGP design tool was able to: (i) take into account the effects of variability on the proposed design; and (ii) yield an optimum design within ASME specifications. However, the solution of the preselected numerical test cases also afforded the opportunity to demonstrate the most compelling attributes of the developed goal programming method, namely: (i) its flexible problem formulation; and (ii) its ability to yield an optimum design suited to a user specified rank ordered priority system.

REFERENCES

1. Vanderplaats, G.N. Numerical Optimization Techniques For Engineering Design. New York: McGraw-Hill, 1984.

2. El-Sayed, M.E., and T.S. Jang. "Structural Optimization with Nonlinear Goal Programming Using Powell's Method." Proceedings of the ASME Design Automation Conference. Chicago, 1990.

3. Lancaster, J. Handbook of Structural Welding. New York: McGraw-Hill, 1992.

4. Kobe Steel, Ltd. Available: http://www.kobelco.co.jp/eneka/p02/tmaine.htm [1998, August 31].

5. Hebeler Corporation. Available: http://www.hebeler.com/asme.htm [1998, August 31].

6. Kempker Associates. Available: http//users.aol.com/Jerkemp/Vessels.html [1998, August 31].

7. Morton Machine Works, Inc. Available: http://www.mortonmachineworks.com/asme.htm [1998, August 31].

8. Chuse, R., and B.E. Carson. Pressure Vessels: The ASME Code Simplified. New York: McGraw-Hill, 1993.

9. Megyesy, E.F. Pressure Vessel Handbook. 10th ed. Tulsa, OK: Pressure Vessel Publishing, Inc., 1995.

10. Funk, E.R., and L.J. Rieber. Handbook of Welding. Belmont, CA: Breton Publishers, 1985.

11. Haftka, R.T., and M.P. Kamat. Elements of Structural Optimization. Dordrecht, The Netherlands: Martinus Nijhoff Publishers, 1985.

12. Xie, Y.M., and G.P. Steven. Evolutionary Structural Optimization. London: Springer-Verlag, 1997.

13. Shigley, J. E., and C.R. Mischke. Mechanical Engineering Design. 5th ed. New York: McGraw-Hill, 1989.

14. Milton, J.S., and J.C. Arnold. Introduction to Probability and Statistics. 3rd ed. New York: McGraw-Hill, 1995.

15. Boresi, A.P., R.J. Schmidt, and O.M. Sidebottom. Advanced Mechanics of Materials. 5th ed. New York: John Wiley & Sons, 1993.

16. Chakravarthy, S.R. MATH 602: Applied Statistics Lecture Notes. Department of Science and Mathematics, Kettering University, 1998.

17. Jang, T.S. "Large Scale Structural Optimization with Linear and Nonlinear Goal Programming." Diss. University of Missouri-Columbia, 1990.